Cellular/Molecular

Erbin Enhances Voltage-Dependent Facilitation of $Ca_v1.3$ Ca^{2+} Channels through Relief of an Autoinhibitory Domain in the $Ca_v1.3$ α_1 Subunit

Irina Calin-Jageman,[1,2] Kuai Yu,[1,2] Randy A. Hall,[1] Lin Mei,[3] and Amy Lee[1,2]

[1]Department of Pharmacology and [2]Center for Neurodegenerative Disease, Emory University, Atlanta, Georgia 30322, and [3]Program of Developmental Neurobiology, Institute of Molecular Medicine and Genetics and Department of Neurology, Medical College of Georgia, Augusta, Georgia 30912

$Ca_v1.3$ (L-type) voltage-gated Ca^{2+} channels have emerged as key players controlling Ca^{2+} signals at excitatory synapses. Compared with the more widely expressed $Ca_v1.2$ L-type channel, relatively little is known about the mechanisms that regulate $Ca_v1.3$ channels. Here, we describe a new role for the PSD-95 (postsynaptic density-95)/Discs large/ZO-1 (zona occludens-1) (PDZ) domain-containing protein, erbin, in directly potentiating $Ca_v1.3$. Erbin specifically forms a complex with $Ca_v1.3$, but not $Ca_v1.2$, in transfected cells. The significance of erbin/$Ca_v1.3$ interactions is supported by colocalization in somatodendritic domains of cortical neurons in culture and coimmunoprecipitation from rat brain lysates. In electrophysiological recordings, erbin augments facilitation of $Ca_v1.3$ currents by a conditioning prepulse, a process known as voltage-dependent facilitation (VDF). This effect requires a direct interaction of the erbin PDZ domain with a PDZ recognition site in the C-terminal domain (CT) of the long variant of the $Ca_v1.3$ α_1 subunit ($\alpha_1$1.3). Compared with $Ca_v1.3$, the $Ca_v1.3$b splice variant, which lacks a large fraction of the $\alpha_1$1.3 CT, shows robust VDF that is not further affected by erbin. When coexpressed as an independent entity with $Ca_v1.3$b or $Ca_v1.3$ plus erbin, the $\alpha_1$1.3 CT strongly suppresses VDF, signifying an autoinhibitory function of this part of the channel. These modulatory effects of erbin, but not $\alpha_1$1.3 CT, depend on the identity of the auxiliary Ca^{2+} channel β subunit. Our findings reveal a novel mechanism by which PDZ interactions and alternative splicing of $\alpha_1$1.3 may influence activity-dependent regulation of $Ca_v1.3$ channels at the synapse.

Key words: **L-type; voltage-gated Ca^{2+} channel; PDZ domain; facilitation; plasticity; excitability**

Introduction

In the nervous system, L-type voltage-gated Ca^{2+} channels play essential roles in controlling membrane excitability (Marrion and Tavalin, 1998), gene expression (Bading et al., 1993; Weick et al., 2003), and synaptic plasticity (Johnston et al., 1992). Of multiple L-type Ca^{2+} channels that have been identified ($Ca_v1.1$–$Ca_v1.4$), $Ca_v1.2$ and $Ca_v1.3$ are widely expressed in the brain and in many of the same neuronal cell groups (Hell et al., 1993b; Ludwig et al., 1997). However, a number of experimental mouse models indicate neural functions for $Ca_v1.3$ that differ from those of $Ca_v1.2$. $Ca_v1.2$ is important for processes underlying spatial memory (Moosmang et al., 2005), whereas $Ca_v1.3$ activation selectively causes depression-like behavior (Sinnegger-Brauns et al., 2004), promotes synaptic changes associated with Parkinson's disease (Day et al., 2006), and is essential for auditory transduction (Platzer et al., 2000; Dou et al., 2004). In addition, Ca^{2+} influx through $Ca_v1.2$ and $Ca_v1.3$ causes transcriptional activation in different brain regions (Hetzenauer et al., 2006). These findings suggest that $Ca_v1.3$ participates in distinct cellular and subcellular tasks compared with $Ca_v1.2$ and therefore may be subject to unique modes of regulation.

In support of this hypothesis, $Ca_v1.3$ but not $Ca_v1.2$ channels interact with Shank, a postsynaptic protein associated with excitatory synapses (Zhang et al., 2005). This interaction targets $Ca_v1.3$ to postsynaptic sites in neurons (Zhang et al., 2005, 2006) and permits $Ca_v1.3$ inhibition by G-protein-coupled receptors (Olson et al., 2005). Shank contains a single PSD-95 (postsynaptic density-95)/Discs large/ZO-1 (zona occludens-1) (PDZ) domain that binds to a C-terminal sequence in the α_1 subunit of $Ca_v1.3$ ($\alpha_1$1.3) (Zhang et al., 2005). Although PDZ domains are generally known to localize and scaffold membrane proteins with intracellular signaling partners, some PDZ interactions directly regulate the gating properties of ion channels (Ou et al., 2003). Given the wealth and diversity of PDZ proteins in the brain (Kim and Sheng, 2004), PDZ partners other than Shank could differentially modulate $Ca_v1.3$ and the role of these channels in various neurobiological contexts.

Here, we identify a novel regulatory mechanism for $Ca_v1.3$ channels involving erbin, a multifunctional PDZ protein concentrated at the neuromuscular junction and at excitatory synapses

Received June 23, 2006; revised Dec. 27, 2006; accepted Dec. 29, 2006.

This work was supported by National Institutes of Health Grants R01 NS044922 (A.L.), T32 DA015040 (I.C.-J.), and R01 NS044521 (L.M.), the W. M. Keck Foundation (R.A.H.), and the Whitehall Foundation (A.L.). We thank Drs. D. Lipscombe and E. Perez-Reyes for $Ca_v1.3$ and β_4 cDNAs, respectively; Dr. Jörg Striessnig for permission to use $Ca_v1.3^{-/-}$ mice; Drs. Geoff Murphy and Anjali Rajadhyaksha for providing $Ca_v1.3^{-/-}$ mouse brains; Amanda Castleberry for preparing the PDZ domain proteomic array used in the initial screen; and Dr. Frank Gordon for advice on statistical analyses.

Correspondence should be addressed to Amy Lee, Department of Pharmacology, Emory University School of Medicine, 5123 Rollins Research Building, 1510 Clifton Road, Atlanta, GA 30322. E-mail: alee@pharm.emory.edu.

DOI:10.1523/JNEUROSCI.5191-06.2007

 0270-6474/07/271374-12$15.00/0

in the CNS (Huang et al., 2001; Kolch, 2003). Erbin binding to the C-terminal domain (CT) of $\alpha_1$1.3 augments voltage-dependent facilitation (VDF) of $Ca_v1.3$ channels containing the auxiliary β_{1b} but not the β_4 subunit by relieving an inhibitory influence of the CT on this process. $Ca_v1.3b$ channels in which the CT is removed by alternative splicing (Safa et al., 2001; Xu and Lipscombe, 2001) show robust VDF that is not further influenced by erbin. Erbin coimmunoprecipitates with and colocalizes with $Ca_v1.3$ in neurons, in which it may regulate postsynaptic $Ca_v1.3$ signaling. Our results define a new role for PDZ proteins in directly modulating $Ca_v1.3$ channels through intermolecular suppression of an autoinhibitory domain in the $\alpha_1$1.3 CT.

Materials and Methods

Constructs and molecular biology. The $\alpha_1$1.3b and $\alpha_1$1.3 variants of the rat brain $Ca_v1.3$ α_1 subunit (GenBank accession numbers AF370009 and AF370010; provided by Dr. D. Lipscombe, Brown University, Providence, RI) and auxiliary channel subunits β_{1b} (GenBank accession number NM017346) or β_4 (GenBank accession number L02315; provided by Dr. E. Perez-Reyes, University of Virginia, Charlottesville, VA) and $\alpha_2\delta$ (GenBank accession number M21948) were used in this study. FLAG-$\alpha_1$1.3 was generated by PCR amplification of a FLAG-tagged fragment (nucleotides 1–660 of $\alpha_1$1.3) and cloned into *Nhe*I and *Ale*I sites of rat $\alpha_1$1.3-pcDNA6/V5-His (Xu and Lipscombe, 2001). FLAG-$\alpha_1$1.2 was described previously (Zhou et al., 2004). For pull-down assays, glutathione *S*-transferase (GST)-tagged constructs containing the cytoplasmic C-terminal domain of rat $\alpha_1$1.3 [GST-$\alpha_1$1.3 CT, nucleotides 5886–6465 (see Fig. 1) and 6360–6465 (see Fig. 8*B*)] or rat $\alpha_1$1.3b [GST-$\alpha_1$1.3b CT, nucleotides 4822–4930 (see Fig. 8*B*)] were subcloned into *Bam*HI/*Not*I sites of pGEX4T.1 (GE Healthcare, Piscataway, NJ). Green fluorescent protein-tagged protein containing the C-terminal 500 aa of $\alpha_1$1.3 not present in $\alpha_1$1.3b (GFP-CT_{500}) corresponds to nucleotides 4903–6465 of rat $\alpha_1$1.3 subcloned into *Hin*dIII/*Sac*II of pEGFPN1 (Clontech, Mountain View, CA). Hexahistidine- and S-tagged constructs (his-S-erbinPDZ, amino acids 1275–1371; his-S-MAGI1PDZ1, amino acids 316–456) were described previously (Fam et al., 2005). Myc-erbin, myc-$erbin_{\Delta PDZ}$, GFP-$erbin_{965}$, and GFP-$erbin_{965\Delta PDZ}$ were also described previously (Huang et al., 2001).

Antibodies. For the generation of rabbit polyclonal $\alpha_1$1.3 antibodies, a GST fusion protein containing amino acids 1–41 (MQHQRQQQED-HANEANYARGTRLPISGEGPTSQPNSSKQTV) of rat $\alpha_1$1.3 (GenBank accession number AF370009), GST-$\alpha_1$1.3 NT_{1-41}, was used as an immunogen, and the resulting antiserum was generated by a commercial source (Covance, Denver, PA). For goat polyclonal $\alpha_1$1.3 antibodies, two peptides corresponding to an N-terminal sequence (amino acids 24–37, PISGEGPTSQPNSS) and a sequence in the cytoplasmic loop linking domains II and III (amino acids 810–827, DNKVTIDDYQEEAEDKD) were used as dual immunogens for antisera generated by a commercial source (ProSci, Poway, CA). The N-terminal sequence was chosen because it shows relatively low sequence homology with the corresponding regions of other L-type channel α_1 subunits (supplemental Fig. 1*A*, available at www.jneurosci.org as supplemental material). The loop II–III sequence was selected because it has been used previously to generate $\alpha_1$1.3-selective antibodies (Hell et al., 1993b). $\alpha_1$1.3 antibodies were purified on affinity columns (AminoLink Coupling Gel; Pierce Biotechnology, Rockford, IL) coupled with the immunogens according to manufacturer's protocol. Rabbit $\alpha_1$1.3 antibodies were purified first by passing antiserum through the GST column to remove anti-GST antibodies, and the flow-through was loaded onto the GST-$\alpha_1$1.3 NT_{1-41} column overnight. Goat $\alpha_1$1.3 antibodies were purified by passing antiserum over a column coupled with both immunogenic peptides. Antibodies were eluted with 5 M $MgCl_2$, dialyzed against PBS, and stored at 4°C in PBS containing 0.02% sodium azide.

The specificity of $\alpha_1$1.3 antibodies was characterized by the following criteria. First, the antibodies recognized $\alpha_1$1.3, but not other L-type channel α_1 subunits, in transfected cell lysates by immunoprecipitation (see Fig. 2*B*), Western blot (supplemental Fig. 1*B*, available at www.jneurosci.org as supplemental material), and immunocytochemistry (supplemental Fig. 1*C*,*D*, available at www.jneurosci.org as supplemental material). Second, these antibodies immunoprecipitated and detected a protein consistent in size with $\alpha_1$1.3 in brain lysates of wild-type mice but not mice with targeted disruption of the $\alpha_1$1.3 gene (Platzer et al., 2000) (see Fig. 2*D*). Third, immunofluorescent staining of primary neurons with both rabbit and goat antibodies was abolished by preadsorption of the antibodies with the immunogen (supplemental Fig. 2*A*,*B*, available at www.jneurosci.org as supplemental material). Together, these results validated the specificity and sensitivity of the antibodies for detection of transfected and native $\alpha_1$1.3 in our experiments.

Rabbit polyclonal $\alpha_1$1.2 antibodies were generated against a peptide corresponding to a sequence in rat $\alpha_1$1.2 (KYTTKINMDDLQPS-ENEDKS) used previously for the generation of $\alpha_1$1.2-specific antibodies (Hell et al., 1993b). The criteria for determining specificity of these antibodies for $\alpha_1$1.2 were similar to those for the $\alpha_1$1.3 antibodies and will be described in a later report. Anti-erbin polyclonal antibodies were produced and characterized previously (Huang et al., 2001).

Other antibodies used were mouse monoclonal antibodies against FLAG M2 and myc (Sigma-Aldrich, St. Louis, MO), GFP (Santa Cruz Biotechnology, Santa Cruz, CA), and HRP-conjugated antibodies against S-protein (Novagen, La Jolla, CA).

Cell culture, transfection, and lysate preparation. A human embryonic kidney cell line transformed with SV40 T antigen (HEK293T) was maintained in DMEM with 10% fetal bovine serum (Invitrogen, Gaithersburg, MD) at 37°C in a humidified atmosphere under 5% CO_2. Cells were grown to 70–80% confluence and transfected using Gene Porter reagent (Gene Therapy Systems, San Diego, CA) according to the manufacturer's protocols. For immunoprecipitation, HEK293T cells were transfected with cDNAs encoding $Ca_v1.2$ (4 μg of FLAG-$\alpha_1$1.2, 2 μg of β_{1b}, and 2 μg of $\alpha_2\delta$) or $Ca_v1.3$ (6 μg of FLAG-$\alpha_1$1.3, 2 μg of β_{1b}, and 2 μg of $\alpha_2\delta$) and myc-erbin (4 μg). For electrophysiological experiments, HEK293T cells plated on 35 mm dishes were transfected with ~5 μg of total DNA (1.5 μg of FLAG-$\alpha_1$1.3 or FLAG-$\alpha_1$1.3b, 0.5 μg of β_{1b} or β_4, and 0.5 μg of $\alpha_2\delta$ with or without 1 μg of erbin) and GFP expression plasmid (0.01 μg) for fluorescent detection of transfected cells.

Pull-down binding assays. GST- or his-S-tagged fusion proteins were prepared and purified on glutathione-agarose beads or Ni^{2+}-nitrilotriacetic acid-agarose beads, respectively, as described previously (Zhou et al., 2004). GST-$\alpha_1$1.3 CT or -$\alpha_1$1.3b CT proteins immobilized on beads were incubated with purified his-S-erbinPDZ or his-S-MAGI1PDZ1 proteins or GFP-$erbin_{965}$-transfected cell lysate and brought to a total volume of 400 μl with binding buffer [50 mM Tris-buffered saline (TBS; 50 mM Tris-HCl, pH 7.5, and 150 mM NaCl)/0.1% Triton X-100/protease inhibitors (1 μg/ml each of PMSF, pepstatin, aprotinin, and leupeptin)]. Binding reactions were incubated, rotating at 4°C for 1–2 h. Beads were washed three times with ice-cold binding buffer (1 ml), and bound proteins were eluted, resolved by SDS-PAGE, and transferred to nitrocellulose. Western blotting was performed with appropriate antibodies followed by HRP-conjugated secondary antibodies and enhanced chemiluminescent detection reagents (GE Healthcare). Ponceau staining was used to verify that equal levels of immobilized GST-$\alpha_1$1.3 CT proteins were used in each experimental group. Interpretations of results from pull-down assays were based on at least three independent experiments.

Coimmunoprecipitation assays. Two days after transfection, lysates from transfected HEK293 cells were harvested and solubilized in 1 ml/100 mm cell culture plate of radioimmunoprecipitation assay (RIPA) buffer (50 mM Tris-HCl, pH 7.5, 150 mM NaCl, 1% NP-40, 0.25% sodium deoxycholate, 1 mM EDTA, and protease inhibitors) at 4°C for 30 min and subjected to centrifugation at 100,000 × *g* (30 min) to remove insoluble material. Lysates were incubated with $\alpha_1$1.3 or $\alpha_1$1.2 antibodies (5 μg) and 50 μl of protein A-Sepharose (50% slurry) for 4 h, rotating at 4°C. After three washes with RIPA buffer (1 ml), proteins were eluted with SDS-containing sample buffer and subjected to SDS-PAGE. Coimmunoprecipitated proteins were detected by Western blotting with specific antibodies as described for pull-down assays. Conclusions were drawn from results of three independent experiments.

For coimmunoprecipitation assays from rat brain, crude membrane fractions were generated as follows: three frozen rat brains were homog-

enized in buffer [(in mM) 320 sucrose, 4 HEPES, 5 EDTA, 5 EGTA, pH 7.4 with NaOH, and protease inhibitors]. After homogenization, large debris was removed by spinning samples at 1000 × *g* for 6 min at 4°C. The supernatant was then subjected to ultracentrifugation at 100,000 × *g* (35 min), and the resulting pellet was solubilized for 3 h in 9 ml of buffer containing 1.2% digitonin, 300 mM KCl, 150 mM NaCl, 10 mM sodium phosphate, pH 7.2, and protease inhibitors at 4°C. A final centrifugation step (100,000 × *g* for 30 min) was performed to remove insoluble material. The resulting supernatant was precleared for 1 h with protein G agarose (200 μl; 50% slurry) and goat IgG (~100 μg). The samples (~9 ml) were then incubated with goat anti-$\alpha_1$1.3 antibodies (~120 μg) or an equivalent amount of goat IgG (final antibody concentration, ~13 μg/ml) and protein G agarose (200 μl; 50% slurry) for 4 h, rotating at 4°C. After three washes with 0.1% digitonin/PBS buffer (1 ml), proteins were eluted with SDS-containing sample buffer and subjected to SDS-PAGE. Coimmunoprecipitated proteins were detected by Western blotting with erbin or rabbit $\alpha_1$1.3-specific antibodies. For immunoprecipitation experiments from brain lysates of $Ca_v1.3^{+/+}$ or $Ca_v1.3^{-/-}$ mice, an identical protocol was used, except that one-half of a mouse brain was used per immunoprecipitation with 30 μg of antibodies. Coimmunoprecipitation experiments from brain tissue were repeated at least twice with consistent results.

Immunocytochemistry. For double-label immunofluorescence, primary cultures of neurons were prepared as follows. Neocortical tissue was dissected from rat embryos (embryonic day 19). The tissue was then digested with papain for 1 h at 37°C and triturated in inactivation solution [minimum essential medium (MEM; Invitrogen) and 10% FBS]. The resulting cell suspension was plated at a density of ~300,000 neurons per 60 mm plate containing glass coverslips precoated with poly-D-lysine. Neurons were maintained in medium containing MEM, 1 mM pyruvate, 0.6% dextrose, 5% FBS, 1× B-27 (Invitrogen), 0.5 mM penicillin/streptomycin/glutamine, and 0.001% MITO+ serum extender (BD Biosciences, San Jose, CA). For immunostaining, coverslips (8–14 d in culture) were fixed in 4% paraformaldehyde/4% sucrose/PBS and incubated in blocking buffer [10% normal goat serum (NGS) or 10% donkey serum (DS), 0.1% Triton X-100, in TBS]. All antibodies were diluted in TBS containing 2.5% NGS or DS and 0.1% Triton X-100, and samples were rinsed three times for 5–10 min between each step. After blocking, samples were incubated with rabbit anti-$\alpha_1$1.3 antibodies (1:50) 4 h to overnight at 4°C and, after rinsing in TBS, with donkey anti-rabbit rhodamine-conjugated Fab fragments (1:300; Jackson ImmunoResearch, West Grove, PA) for 60 min. Sections were rinsed and blocked with goat anti-rabbit Fab fragments (1:50; Jackson ImmunoResearch) for ~2.5 h to block any rabbit IgG sites before the second labeling step. Sections were then incubated overnight at 4°C with anti-erbin antibodies (1:100–1:400), rinsed, and incubated with donkey FITC–anti-rabbit IgG (1:300; Jackson ImmunoResearch). The double-labeled sections were mounted and coverslipped with Vectashield (Vector Laboratories, Burlingame, CA) for viewing on a Zeiss (Oberkochen, Germany) LSM510 Meta confocal microscope. Image processing was with Zeiss LSM Image Browser and Adobe Photoshop (Adobe Systems, San Jose, CA) software.

Because the double-labeling procedure involved two rabbit antibodies, a number of control experiments were performed to confirm the pattern of erbin and $\alpha_1$1.3 colocalization. In particular, to ensure that the incubation with goat anti-rabbit Fab fragments was sufficient to prevent recognition of the first primary antibody ($\alpha_1$1.3) by the second secondary antibody (FITC–anti-rabbit IgG), anti-erbin antibodies were omitted (supplemental Fig. 2, available at www.jneurosci.org as supplemental material). Loss of FITC fluorescence in this control experiment (supplemental Fig. 2*D*, available at www.jneurosci.org as supplemental material) argued against the possibility that overlap in $\alpha_1$1.3 and erbin immunofluorescence resulted from insufficient blocking and therefore reactivity of both secondary antibodies with $\alpha_1$1.3-labeled sites. Interpretations from immunocytochemical experiments were based on consistent results obtained from more than five independent experiments.

Electrophysiological recordings. At least 48 h after transfection, whole-cell patch-clamp recordings of transfected cells were acquired with a HEKA Elektronik (Lambrecht/Pfalz, Germany) EPC-9 patch-clamp amplifier. Data acquisition and leak subtraction using a P/−4 protocol were done with Pulse software (HEKA Elektronik). Extracellular recording solutions contained the following (in mM): 150 Tris, 1 $MgCl_2$, and 10 $BaCl_2$ or 10 $CaCl_2$. Intracellular solutions consisted of the following (in mM): 140 *N*-methyl-D-glucamine, 10 HEPES, 2 $MgCl_2$, 2 Mg-ATP, and 5 EGTA. The pH of intracellular and extracellular recording solutions was adjusted to 7.3 with methanesulfonic acid. Electrode resistances were typically 1–2 MΩ in the bath solution, and series resistance was ~2–4 MΩ, compensated up to 80%. Normalized tail current–voltage and prepulse voltage-dependence data were fit with a single Boltzmann function: $A/\{1 + \exp[(V - V_{1/2})/k] + b\}$, where V is the test or prepulse voltage, $V_{1/2}$ is the half-maximal voltage, k is a slope factor, A is the amplitude, and b is the baseline. Curve fits and data analyses were done with Igor Pro software (Wavemetrics, Lake Oswego, OR). All averaged data are presented as the mean ± SEM. Statistical significance of differences between two groups was determined by Student's *t* test as indicated (SigmaPlot; Systat Software, San Jose, CA). For statistical analyses of prepulse voltage and *I–V* curves, data were compared by two-way repeated-measures ANOVA (SigmaStat; Systat Software).

Results

Erbin binds to the $\alpha_1$1.3 C-terminal domain

The extreme C-terminal residues of $\alpha_1$1.3 (ITTL) (Fig. 1*A*) are consistent with a signature sequence favored by class I PDZ domains, (S/T)-X-ϕ-COOH, where ϕ is a hydrophobic amino acid, and X is any amino acid (Songyang et al., 1997). To identify PDZ proteins interacting with this sequence in $\alpha_1$1.3, we used a GST fusion protein containing the last 200 aa of $\alpha_1$1.3 CT (Fig. 1*A*) to screen a proteomic array of 96 putative class I PDZ domains, as described previously (Fam et al., 2005). Several PDZ domains on the array interacted with $\alpha_1$1.3 (data not shown), including one belonging to erbin, a member of the LAP (leucine-rich region and PDZ) family (Borg et al., 2000; Huang et al., 2001) (Fig. 1*B*). The interaction between erbin and $\alpha_1$1.3 was confirmed in a pull-down assay with immobilized GST-$\alpha_1$1.3 CT and a truncated version of erbin containing the PDZ domain (GFP-$erbin_{965}$) (Fig. 1*C*). GST-$\alpha_1$1.3 CT, but not the GST control, precipitated GFP-$erbin_{965}$ from transfected cell lysates (Fig. 1*C*). To discount the possibility that GFP-$erbin_{965}$ could have associated indirectly with $\alpha_1$1.3 CT via a second protein in the transfected cell lysate, we performed pull-down assays with purified protein corresponding to the PDZ domain of erbin (erbinPDZ) (Fig. 1*D*). Although GST-$\alpha_1$1.3 CT showed dose-dependent binding to erbinPDZ, the class I PDZ of a different protein [membrane-associated guanylate kinase inverted 1 (MAGI1)] did not bind to GST-$\alpha_1$1.3 CT (Fig. 1*D*). These results confirm that $\alpha_1$1.3 CT interacts directly and specifically with the PDZ domain of erbin.

Although most PDZ domains interact with a canonical sequence at the extreme CT of their ligands, some also recognize internal motifs not at the CT (Penkert et al., 2004). Because the GST-$\alpha_1$1.3 CT fusion protein encompassed a relatively large region (~200 aa) (Fig. 1*A*), binding to erbin could have been mediated by residues other than the C-terminal PDZ recognition site. To confirm the importance of the PDZ signature sequence (ITTL) in $\alpha_1$1.3 CT for binding to erbin, we tested how substitution of alanine for the final leucine in this sequence affected the interaction ($\alpha_1$1.3 $CT_{L–A}$) (Fig. 1*E*). This substitution eliminates the hydrophobic nature of the final residue, which is critical for maintaining PDZ–ligand interactions (Songyang et al., 1997). If erbin binds to $\alpha_1$1.3 CT via a conventional class I PDZ interaction, the L–A substitution should significantly weaken the interaction with erbin. Consistent with this prediction, binding of erbinPDZ to GST-$\alpha_1$1.3 $CT_{L–A}$ was greatly reduced relative to GST-$\alpha_1$1.3 in pull-down experiments (Fig. 1*E*). Therefore, erbin binding to $\alpha_1$1.3 CT depends on the C-terminal PDZ recognition site.

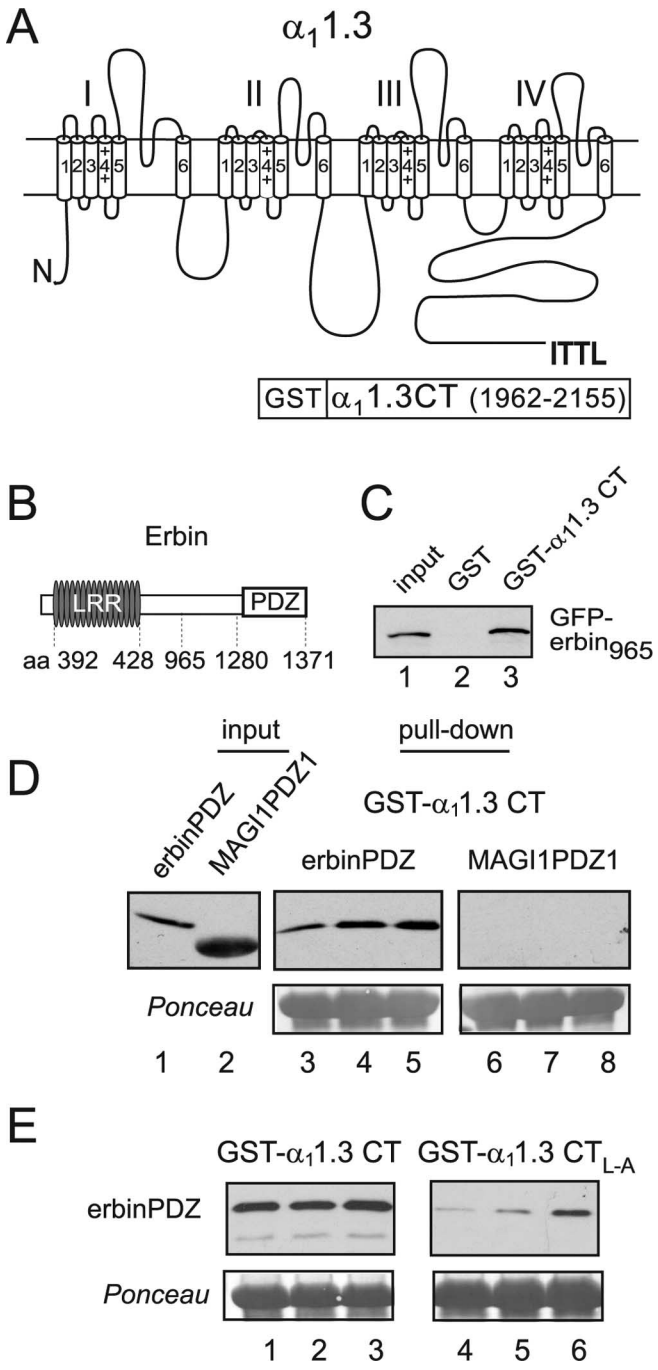

Figure 1. The PDZ domain of erbin binds to the C-terminal domain of $\alpha_1$1.3. ***A***, Schematic of rat $\alpha_1$1.3 showing class I PDZ-binding consensus sequence (ITTL) in the cytoplasmic C-terminal domain and the region used for GST-$\alpha_1$1.3 CT in pull-down assays (amino acids 1962–2155). ***B***, Schematic of mouse erbin indicating position of LRR (amino acids 392–428) and the PDZ domain (amino acids 1280–1371). ***C***, Binding of erbin to $\alpha_1$1.3 CT. GST-$\alpha_1$1.3 CT (lane 3) or GST alone (lane 2) was immobilized on glutathione-agarose beads and incubated with lysates from cells transfected with GFP-$erbin_{965}$ (amino acids 965–1371). Bound GFP-$erbin_{965}$ was detected by Western blot with anti-GFP antibodies. Lane 1 shows ~15% of GFP-$erbin_{965}$ input used in the pull-down assay. ***D***, Binding of erbinPDZ but not MAGI1PDZ1 to $\alpha_1$1.3 CT. GST-$\alpha_1$1.3 CT was incubated with purified his-S-erbinPDZ (lanes 3–5) or his-S-MAGI1PDZ1 (lanes 6–8). Input his-S-tagged protein was the following (in μg): 1 (lanes 3, 6), 2 (lanes 4, 7), and 4 (lanes 5, 8). Input lanes 1 and 2 show his-S-tagged proteins used in the assay (1 μg). ***E***, Impaired binding of erbinPDZ to $\alpha_1$1.3 CT_{L-A}. His-S-erbinPDZ protein (lanes 1, 4, 1.5 μg; lanes 2, 5, 3 μg; lanes 3, 6, 6 μg) was incubated with GST-$\alpha_1$1.3 CT (lanes 1–3) or GST-$\alpha_1$1.3 CT_{L-A} (lanes 4–6). In ***D*** and ***E***, bound proteins were detected by Western blot (top) with anti-S-protein antibodies, and Ponceau staining (bottom) shows equal levels of GST-$\alpha_1$1.3 CT or GST-$\alpha_1$1.3 CT_{L-A} in each group.

To confirm that erbin interacts not only with the isolated CT fragment of $\alpha_1$1.3 but also with the intact channel in mammalian cells, coimmunoprecipitation experiments were performed with lysates of HEK293T cells cotransfected with $Ca_v1.3$ subunits (FLAG-$\alpha_1$1.3, β_{1b}, and $\alpha_2\delta$) and myc-tagged erbin. Because the α_1 subunit of $Ca_v1.2$ ($\alpha_1$1.2) also contains a class I PDZ-binding element (VSNL) (Fig. 2*A*), we determined whether myc-erbin might selectively interact with either channel. Using $\alpha_1$1.3 antibodies, we found that myc-erbin coimmunoprecipitated with $\alpha_1$1.3 (Fig. 2*B*, lane 1). Myc-erbin was not detected when $\alpha_1$1.3 antibodies were applied to lysates from cells cotransfected with $\alpha_1$1.2 and erbin, arguing against nonspecific immunoprecipitation of erbin by $\alpha_1$1.3 antibodies (Fig. 2*B*, lane 2). This result also confirmed that the antibodies specifically recognized $\alpha_1$1.3 and not $\alpha_1$1.2. However, the amount of myc-erbin that coimmunoprecipitated with $Ca_v1.3$ was relatively small (lane 1) compared with the total amount of myc-erbin that was detected in the cell lysates (lane 6). This could be explained by the presence of erbin endogenously expressed in HEK293 cells (Huang et al., 2001), which might have competed with transfected myc-erbin for interacting with $Ca_v1.3$. In addition, previous analyses indicate that the erbin PDZ domain has a strong preference for ligands with the CT sequence (E/D)-(S/T/V)-X-V and binds relatively weakly to sequences more similar to the ITTL $\alpha_1$1.3 motif (Jaulin-Bastard et al., 2001). Such low-affinity interactions might be difficult to maintain during immunoprecipitation procedures that required strong detergent solubilization conditions.

With $\alpha_1$1.2 antibodies, myc-erbin could not be coimmunoprecipitated with $\alpha_1$1.2, despite the fact that $\alpha_1$1.2 expression and immunoprecipitation was consistently greater than that observed for $\alpha_1$1.3 (Fig. 2*B*, lanes 1, 3, 5, 6). The $\alpha_1$1.2 antibodies did not immunoprecipitate $\alpha_1$1.3, confirming the specificity of these antibodies for $\alpha_1$1.2 (Fig. 2*B*, lane 2). Inability of myc-erbin to coimmunoprecipitate with $\alpha_1$1.2 was not related to insufficient levels of myc-erbin, because Western blots of the transfected cell lysates indicated that equal levels of myc-erbin were coexpressed with $Ca_v1.3$ and $Ca_v1.2$ (Fig. 2*B*, lanes 5, 6). These results confirm that erbin selectively forms a complex with $Ca_v1.3$ channels and support previous observations that $Ca_v1.2$ and $Ca_v1.3$ are distinguished by the types of PDZ proteins with which they interact (Weick et al., 2003; Zhang et al., 2005).

$Ca_v1.3$ and erbin coimmunoprecipitate and colocalize in neurons

To address the neurobiological significance of erbin/$Ca_v1.3$ interactions, we determined whether erbin and $Ca_v1.3$ formed a complex in rat brain in coimmunoprecipitation experiments. $Ca_v1.3$ channels were immunoprecipitated from solubilized rat brain membrane fractions with goat polyclonal $\alpha_1$1.3 antibodies. $Ca_v1.3$ and associated erbin were detected by Western blot with rabbit polyclonal $\alpha_1$1.3 and erbin antibodies, respectively. In these experiments, erbin was coimmunoprecipitated with $\alpha_1$1.3 using $\alpha_1$1.3 antibodies (Fig. 2*C*). The coimmunoprecipitation was specific in that a similar result was not obtained with an equivalent concentration of control IgG (Fig. 2*C*). The ~200 kDa protein immunoprecipitated and immunoblotted with our $\alpha_1$1.3 antibodies corresponded to $\alpha_1$1.3, because it was observed in brain lysates from wild-type mice ($Ca_v1.3^{+/+}$) but not mice lacking $\alpha_1$1.3 ($Ca_v1.3^{-/-}$) (Fig. 2*D*), which were characterized previously (Platzer et al., 2000). These results confirm the existence of erbin and $Ca_v1.3$ interactions in the brain.

If erbin is a significant partner of neuronal $Ca_v1.3$ channels, these proteins should show similar cellular and subcellular local-

ization in the brain. To test this, we used confocal microscopy and double-label immunofluorescence of cortical neurons in culture. We observed erbin and $Ca_v1.3$ immunofluorescence in neuronal cell bodies (Fig. 3*A–C*,*G–I*). In addition, punctate erbin and $Ca_v1.3$ immunofluorescence was observed in proximal dendrites (Fig. 3*D–F*). In developing neurons, erbin and $Ca_v1.3$ immunofluorescence coincided strongly at the distal ends of dendritic processes (Fig. 3*G–I*). Colocalization of erbin and $Ca_v1.3$ in the soma and proximal dendrites was extensive in virtually all neurons examined (Fig. 3*C*,*F*,*I*). However, colocalization of erbin and $Ca_v1.3$ was not complete, and there were many puncta that showed only $Ca_v1.3$ or erbin labeling (Fig. 3*D–F*). In addition to control experiments (supplemental Fig. 2, available at www.jneurosci.org as supplemental material), these results discounted the possibility that overlapping fluorescence was artifactual as a result of cross-reactivity of the secondary reagents in the double-labeling protocol. The nucleus of most neurons was labeled with erbin but not $Ca_v1.3$ antibodies (Fig. 3*A–C*,*G–I*), which is not unexpected, because erbin is involved in multiple cellular signaling functions (Kolch, 2003). Nevertheless, the strong colocalization of erbin and $Ca_v1.3$ in neurons and coimmunoprecipitation from brain lysates support the potential for erbin to physiologically interact with neuronal $Ca_v1.3$ channels.

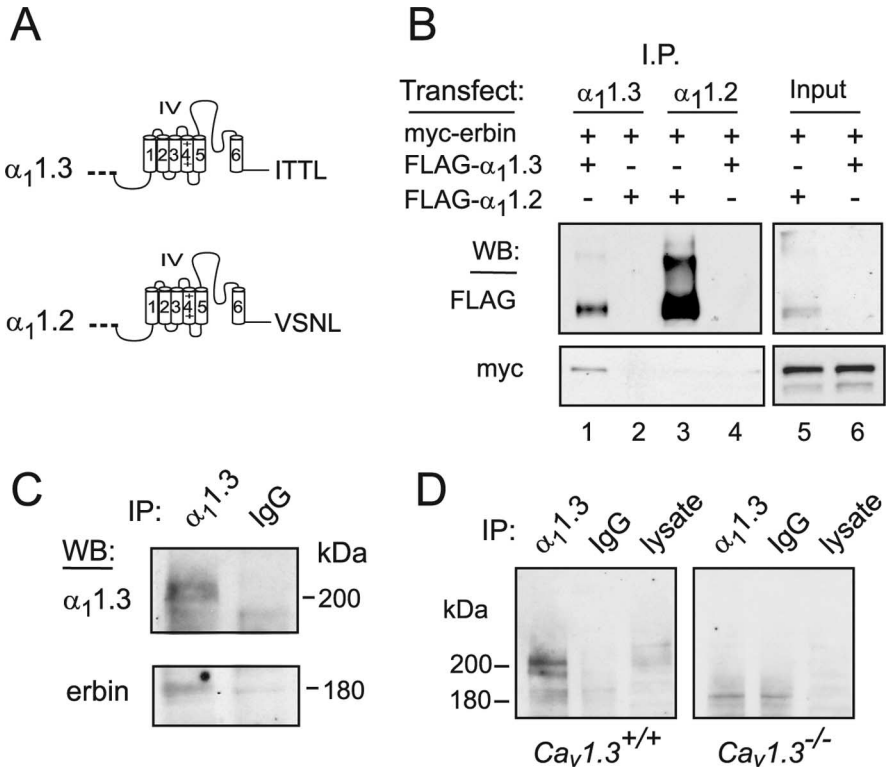

Figure 2. Coimmunoprecipitation of erbin with $Ca_v1.3$ from transfected cells and brain. ***A***, Schematic of $\alpha_1 1.3$ and $\alpha_1 1.2$ showing C-terminal PDZ-binding motifs. ***B***, Coimmunoprecipitation of erbin and $Ca_v1.3$ from transfected cells. HEK293T cells were cotransfected with myc-erbin and $Ca_v1.3$ (FLAG-$\alpha_1 1.3$, β_{1b}, and $\alpha_2\delta$; lanes 1, 4, 6) or $Ca_v1.2$ (FLAG-$\alpha_1 1.2$, β_{1b}, and $\alpha_2\delta$; lanes 2, 3, 5) and subjected to lysis and immunoprecipitation using rabbit antibodies against $\alpha_1 1.3$ (lanes 1, 2) or $\alpha_1 1.2$ (lanes 3, 4). Immunoprecipitated proteins (I.P.; lanes 1–4) were detected by Western blotting (WB) with antibodies recognizing FLAG (top) or myc (bottom) epitopes. Lanes 5 and 6 represent 5% of the cell lysate input used for coimmunoprecipitation. ***C***, Coimmunoprecipitation of erbin and $Ca_v1.3$ from the brain. Rat brain lysates were incubated with goat $\alpha_1 1.3$ antibodies or control goat IgG for immunoprecipitation, and $\alpha_1 1.3$ and erbin were detected by Western blotting with rabbit $\alpha_1 1.3$ and erbin antibodies, respectively. ***D***, Lack of $\alpha_1 1.3$ immunoprecipitation in $Ca_v1.3^{-/-}$ mouse brain. $\alpha_1 1.3$ immunoprecipitation protocol used in ***C*** was applied to brain lysates from $Ca_v1.3^{+/+}$ or $Ca_v1.3^{-/-}$ mice. An ~200 kDa protein corresponding to $\alpha_1 1.3$ was detected in the brain lysate, and samples were immunoprecipitated with $\alpha_1 1.3$ antibodies from $Ca_v1.3^{+/+}$ but not $Ca_v1.3^{-/-}$ mice. Lysate lanes represent 3% of the input used for coimmunoprecipitation.

Erbin augments voltage-dependent facilitation of $Ca_v1.3$

The cytoplasmic C-terminal domain of the $Ca_v1.2$ α_1 subunit interacts with a variety of regulatory proteins that directly modulate channel activation or inactivation (Catterall, 2000). To test the hypothesis that erbin binding to $\alpha_1 1.3$ CT might similarly influence the function of $Ca_v1.3$, we screened for modulatory effects of erbin in electrophysiological recordings of HEK293T cells cotransfected with $Ca_v1.3$ subunits ($\alpha_1 1.3$, β_{1b}, and $\alpha_2\delta$). This system allows transfection and electrophysiological analysis of recombinant channels in the relative absence of competing influences. Similar experiments in primary neurons are complicated by the existence of multiple classes of voltage-gated Ca^{2+} channels and subsequent difficulty of isolating modulatory effects specific for $Ca_v1.3$ channels. Despite the low levels of endogenous erbin in HEK293 cells (Huang et al., 2001), functional effects of erbin on signaling have been studied in this cell line through transfection of exogenous erbin cDNAs (Dai et al., 2006), which we found to increase erbin expression significantly over endogenous levels (data not shown). Therefore, modulatory effects of erbin could be resolved by comparing $Ca_v1.3$ properties in cells cotransfected with $Ca_v1.3$ and erbin and in cells transfected with $Ca_v1.3$ alone.

Consistent with previous reports (Koschak et al., 2001; Safa et al., 2001; Scholze et al., 2001; Xu and Lipscombe, 2001), $Ca_v1.3$ showed a relatively hyperpolarized range of activation (Fig. 4). However, parameters for tail current activation curves were not significantly different in cells transfected with $Ca_v1.3$ alone ($V_{1/2} = -21.7 \pm 1.6$ mV; $k = -5.8 \pm 0.5$; $n = 9$) and those cotransfected with erbin ($V_{1/2} = -22.7 \pm 1.9$ mV; $k = -6.8 \pm 0.7$; $n = 6$; $p = 0.70$ for $V_{1/2}$; $p = 0.25$ for k) (Fig. 4*A*,*B*). In addition, erbin did not influence the average amplitude of the $Ca_v1.3$ peak current evoked by various test voltages (Fig. 4*C*,*D*). There was no significant difference in the peak current amplitudes in current–voltage (*I–V*) relationships in cells transfected with $Ca_v1.3$ alone and those cotransfected with erbin ($F_{(1,12)} = 0.0005$; $p = 0.983$) (Fig. 4*C*,*D*). These results show that erbin does not regulate the expression level or activation properties of $Ca_v1.3$ channels in mammalian cells.

$Ca_v1.3$ channels undergo prominent VDF that, in recombinant systems, is independent of heterotrimeric G-proteins or phosphorylation (Safa et al., 2001). To determine whether erbin influenced this aspect of $Ca_v1.3$ function, we used a paired-pulse protocol in which the amplitude of two test currents (P1 and P2) evoked by the same voltage step was compared before and after a conditioning (facilitating) prepulse (Fig. 5*A*). Consistent with previous studies (Safa et al., 2001), a short (20 ms) conditioning prepulse from −90 to +60 mV caused a significant increase ($30.3 \pm 4.1\%$; $n = 12$; $p < 0.01$) in $Ca_v1.3$ currents evoked by a test pulse from −90 to −20 mV (Fig. 5*A*). With the same voltage

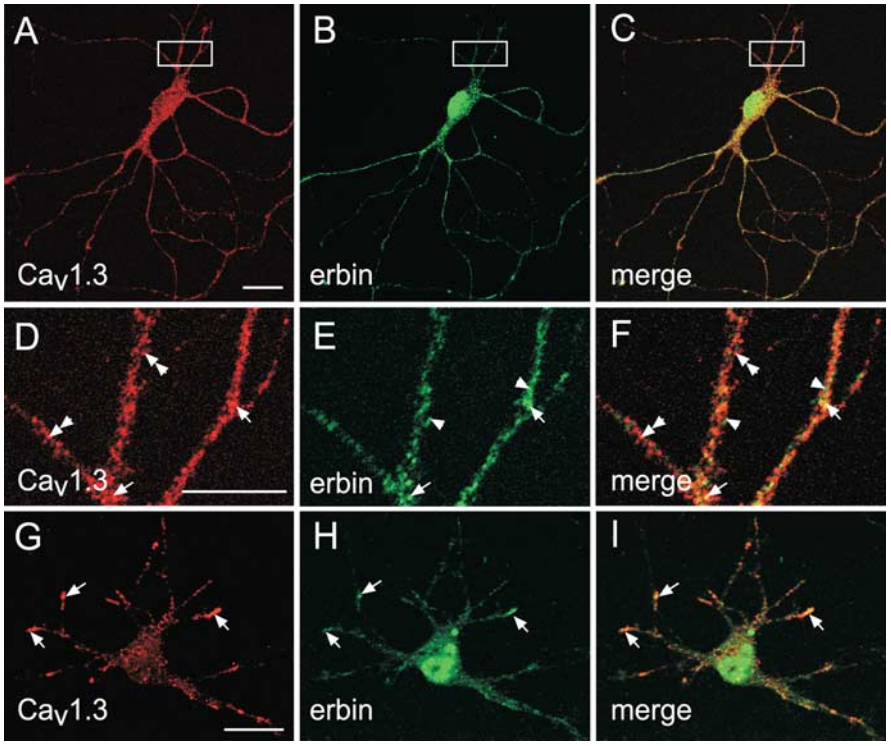

Figure 3. $Ca_v1.3$ and erbin colocalize in somatodendritic domains of cortical neurons in culture. ***A–I***, Confocal images of primary cortical neuron cultures (***A–F***, 14 d in culture; ***G–I***, 8 d in culture) sequentially double labeled with antibodies against $\alpha_1$1.3 (to detect $Ca_v1.3$) and erbin are shown. Immunofluorescence was viewed under optics for rhodamine for $Ca_v1.3$ (***A***, ***D***, ***G***) or fluorescein for erbin (***B***, ***E***, ***H***). Regions of colocalization appear yellow in the merged images (***C***, ***F***, ***I***). Extensive colocalization of erbin and $Ca_v1.3$ was detected in cell bodies (***A–C***, ***G–I***) and dendrites (***D–F***; higher-magnification view of boxed region in panels ***A–C***). In ***D–I***, elements immunoreactive for $Ca_v1.3$ alone (double arrowheads), erbin alone (arrowheads), or $Ca_v1.3$ plus erbin (arrows) are indicated. Scale bars: ***A*** (for ***A–C***), ***G*** (for ***G–I***), 20 μm; (in ***D***) ***D–F***, 10 μm.

protocol, the amount of facilitation in cells cotransfected with erbin was dramatically increased (47.8 ± 6.6%; $n = 10$) and was significantly greater than in cells transfected with $Ca_v1.3$ alone ($p < 0.01$) (Fig. 5*A*). The enhanced facilitation attributable to erbin could have resulted from a negative shift or steeper dependence of facilitation on prepulse voltage. To test this, we compared the relationship between prepulse voltage and percentage of maximal facilitation in cells transfected with $Ca_v1.3$ alone or those cotransfected with erbin (Fig. 5*B*). However, Boltzmann fits of prepulse voltage curves revealed no significant effect of erbin on either $V_{1/2}$ (−12.2 ± 3.4 for $Ca_v1.3$ alone vs −8.3 ± 3.4 for $Ca_v1.3$ plus erbin; $p = 0.62$) or slope (−19.0 ± 2.7 for $Ca_v1.3$ alone vs −17.6 ± 1.7 for $Ca_v1.3$ plus erbin; $p = 0.71$). A second mechanism by which erbin could augment VDF is by increasing the number of channels undergoing facilitation as a result of a given prepulse. This was tested by plotting net facilitation, which was the amplitude of the P2 relative to the P1 current [F_{ratio} (P2/P1)] (Fig. 5*C*) against prepulse voltage. With prepulse voltages ranging from −20 to +60 mV, net facilitation was significantly greater ($F_{(1,20)} = 5.25$; $p < 0.05$) in cells cotransfected with erbin than in cells with $Ca_v1.3$ alone (Fig. 5*C*). These results confirm that erbin promotes VDF by increasing the pool of channels undergoing prepulse-induced facilitation, rather than enhancing voltage dependence of entry into the facilitated state.

In these experiments, Ba^{2+} rather than Ca^{2+} was used as the charge carrier to resolve VDF without the competing effects of Ca^{2+}-dependent inactivation, which would significantly diminish the amplitude of the P2 test current in double-pulse protocols. However, because Ca^{2+} is the physiologically relevant charge carrier, we also tested whether erbin influenced facilitation of $Ca_v1.3$ Ca^{2+} currents (Fig. 6). With a modified double-pulse protocol, Ca^{2+}-dependent inactivation of $Ca_v1.3$ currents was evident as a decrease in the P2 relative to the P1 current ($F_{ratio} < 1$) with prepulse voltages ranging from −20 to +30 mV (Fig. 6*B*). As would be expected of a Ca^{2+}-dependent process, inactivation paralleled the amount of Ca^{2+} influx during the prepulse such that F_{ratio} was smallest with a prepulse to 0 mV (Fig. 6*B*), which evoked the maximal inward Ca^{2+} current (data not shown). Although erbin did not affect the extent to which $Ca_v1.3$ Ca^{2+} currents inactivated ($p > 0.18$, for prepulses from −40 mV to +30 mV), prepulse steps from +50 to +80 mV caused facilitation ($F_{ratio} > 1$) of $Ca_v1.3$ Ca^{2+} currents that was significantly greater ($p < 0.05$) in cells cotransfected with erbin than in cells with $Ca_v1.3$ alone (Fig. 6*A*,*B*). That erbin increased facilitation across this voltage range for $Ca_v1.3$ when either Ca^{2+} (Fig. 6) or Ba^{2+} (Fig. 5) was used as the permeant ion supports modulation of voltage- rather than Ca^{2+}-dependent facilitation. As for $Ca_v1.3$ Ba^{2+} currents, the effect of erbin on facilitation of Ca^{2+} currents was not accompanied by effects on current amplitude, because *I–V* relationships for Ca^{2+} currents in cells with $Ca_v1.3$ alone and $Ca_v1.3$ plus erbin were not significantly different ($p = 0.16$; data not shown). Because the effects of erbin on facilitation of $Ca_v1.3$ Ca^{2+} currents were smaller and occurred across a narrower set of prepulse voltages than for Ba^{2+} currents, the molecular mechanism underlying erbin-dependent increases in VDF was analyzed further with Ba^{2+} as the charge carrier.

Erbin binding to $\alpha_1$1.3 supports VDF of $Ca_v1.3$

Based on our biochemical evidence supporting a direct interaction between erbin and $\alpha_1$1.3 (Figs. 1, 2), we hypothesized that this interaction is required for the modulation of $Ca_v1.3$ VDF by erbin. If so, then preventing erbin from binding to $\alpha_1$1.3 should abolish the increased VDF in cells with $Ca_v1.3$ plus erbin. This prediction was first tested with truncated erbin constructs that either lacked or were generally restricted to the PDZ domain ($erbin_{\Delta PDZ}$ and $erbin_{965}$, respectively) (Fig. 7). Compared with cells cotransfected with full-length erbin, VDF was significantly reduced when $Ca_v1.3$ was cotransfected with $erbin_{\Delta PDZ}$ ($F_{(1,16)} = 6.46$; $p < 0.05$) (Fig. 7*A*,*B*). This result confirms the importance of the erbin PDZ domain for VDF. However, erbin contains other functional domains, including a leucine-rich repeat region (LRR) (Fig. 1*B*) implicated in subcellular trafficking of membrane proteins (Legouis et al., 2003). Thus, it was possible that the PDZ domain acted in concert with the LRR of erbin to promote VDF of $Ca_v1.3$ through a mechanism independent of binding to $\alpha_1$1.3. This was not the case, because $erbin_{965}$, which did not contain the LRR, caused increased VDF compared with cells with $Ca_v1.3$ alone ($F_{(1,15)} = 5.44$; $p < 0.05$) (Fig. 7*A*,*C*). Moreover, the effect of $erbin_{965}$ on VDF was not significantly different from full-length erbin ($F_{(1,13)} = 0.05$; $p = 0.83$) (Fig. 7*C*). These results

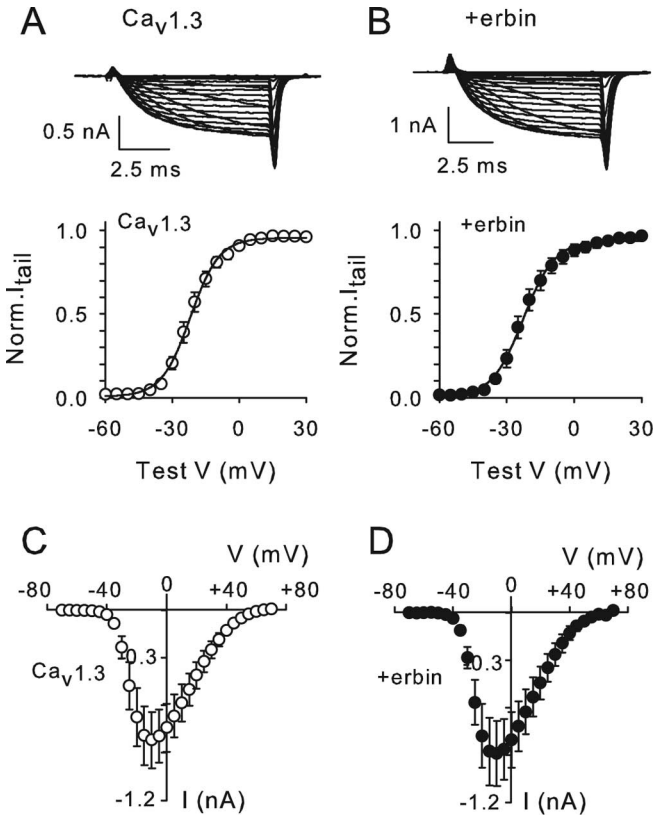

Figure 4. Erbin does not affect voltage-dependent activation or mean amplitude of $Ca_v1.3$ currents. ***A***, ***B***, Normalized tail current (Norm. I_{tail}) activation curves for HEK293T cells transfected with $Ca_v1.3$ alone ($n = 9$) (***A***) or cotransfected with $Ca_v1.3$ plus erbin ($n = 6$) (***B***). Test pulses (10 ms) were applied from a holding voltage of −90 mV to various voltages, and peak tail currents were measured after repolarization to −70 mV for 2 ms. Tail currents were normalized to the largest in the series and plotted against test voltage. Representative current traces are shown at top. ***C***, ***D***, Current–voltage relationships for $Ca_v1.3$ alone (***C***) and $Ca_v1.3$ plus erbin (***D***). Data were from same voltage protocol as in ***A*** and ***B***, except that peak current amplitudes during the test pulse were plotted against test voltage. Error bars represent SEM.

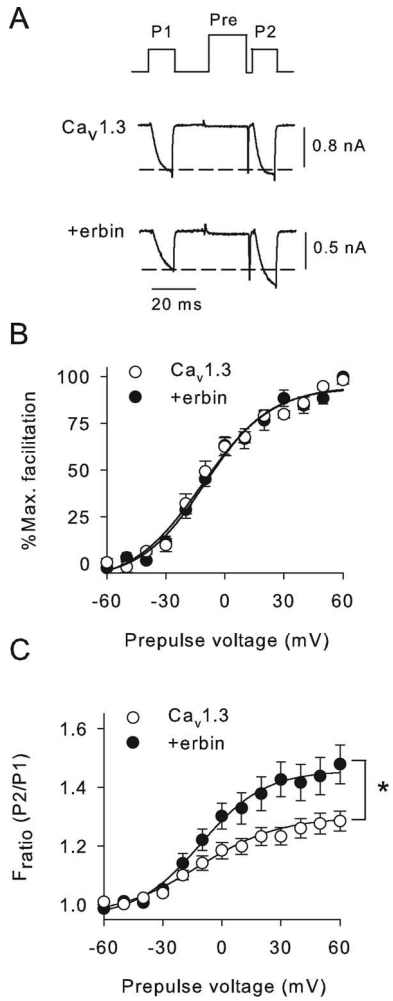

Figure 5. Erbin augments VDF of $Ca_v1.3$ Ba^{2+} currents. ***A***, Representative Ba^{2+} current traces and double-pulse voltage protocol for measuring VDF in cells transfected with $Ca_v1.3$ alone or cotransfected with erbin. Currents were evoked by 10 ms test pulses from −90 to −20 mV before (P1) and after (P2) a conditioning 20 ms prepulse (Pre) to +60 mV. ***B***, No effect of erbin on prepulse voltage dependence of facilitation. Percentage of facilitation was calculated as $[(I_{P2}/I_{P1}) - 1] \times 100$ for cells for different prepulse voltages, normalized to that for a +60 mV prepulse, and plotted as percentage of maximum (Max.) facilitation against prepulse voltage for cells transfected with $Ca_v1.3$ alone ($n = 11$) or cotransfected with erbin ($n = 10$). ***C***, Increased net facilitation attributable to erbin. F_{ratio} represents the ratio of the P2 and P1 test currents and is plotted against prepulse voltage for $Ca_v1.3$ alone ($n = 12$) or $Ca_v1.3$ plus erbin ($n = 10$). *$p < 0.05$. Error bars represent SEM.

show that the PDZ domain of erbin is necessary and sufficient for modulation of $Ca_v1.3$ VDF.

To characterize the importance of the PDZ-binding site in the $\alpha_1$1.3 CT for erbin modulation, we took advantage of a naturally occurring $\alpha_1$1.3 variant ($\alpha_1$1.3b) in which inclusion of an alternatively spliced exon leads to truncation of the C-terminal domain and subsequent elimination of the PDZ-binding sequence (Safa et al., 2001; Xu and Lipscombe, 2001) (Fig. 8*A*). If erbin binding specifically to $\alpha_1$1.3 CT was required for increasing VDF, channels containing $\alpha_1$1.3b ($Ca_v1.3b$) should be insensitive to the effects of cotransfected erbin. The potential of erbin to interact with $\alpha_1$1.3b was first tested in pull-down assays with his-tagged erbinPDZ and GST-tagged $\alpha_1$1.3 CT or $\alpha_1$1.3b CT (Fig. 8*A*). Relatively weak binding of erbinPDZ was observed with $\alpha_1$1.3b CT compared with $\alpha_1$1.3 CT (Fig. 8*B*). Consistent with these results, VDF of $Ca_v1.3b$ channels was not significantly affected by cotransfected erbin ($F_{(1,20)} = 0.06$; $p = 0.81$) (Fig. 8*C*). This was not attributable to the inability of $Ca_v1.3b$ channels to undergo VDF, because VDF was quite robust in cells transfected with $Ca_v1.3b$ alone ($F_{ratio} = 1.42 \pm 0.09$ with a +60 mV prepulse; $n = 14$). Together, our results support a mechanism in which the PDZ domain of erbin binding to the C-terminal domain $\alpha_1$1.3 mediates enhanced VDF that is specific for $Ca_v1.3$ L-type channels.

Erbin relieves the inhibitory effect of $\alpha_1$1.3 CT on VDF

In recordings of the short $Ca_v1.3b$ variant, we found that VDF was on average greater than for $Ca_v1.3$ and was not different from that caused by erbin in cells cotransfected with the long $Ca_v1.3$ variant ($F_{(1,22)} = 0.04$; $p = 0.85$) (Figs. 5*C*, 8*C*). This result suggested an intriguing mechanism in which the $\alpha_1$1.3 CT, which is missing in $Ca_v1.3b$, may act as an inhibitory module for VDF. The absence of the inhibitory CT domain in $\alpha_1$1.3b might therefore permit enhanced facilitation of $Ca_v1.3b$, which cannot be influenced further by erbin (Fig. 8*C*). If so, then $\alpha_1$1.3 CT when expressed as a separate entity should suppress VDF of $Ca_v1.3b$. We tested this prediction with GFP-CT_{500} (Fig. 9). Compared with cells with $Ca_v1.3b$ alone, VDF was significantly impaired by cotransfection with CT_{500} ($F_{(1,16)} = 14.32$; $p < 0.01$) (Fig. 9*A*). In contrast, CT_{500} did not significantly affect VDF for $Ca_v1.3$ ($F_{(1,6)} = 0.49$; $p = 0.51$) (Fig. 9*B*). These results confirm an inhibitory role for the CT of $\alpha_1$1.3 in VDF.

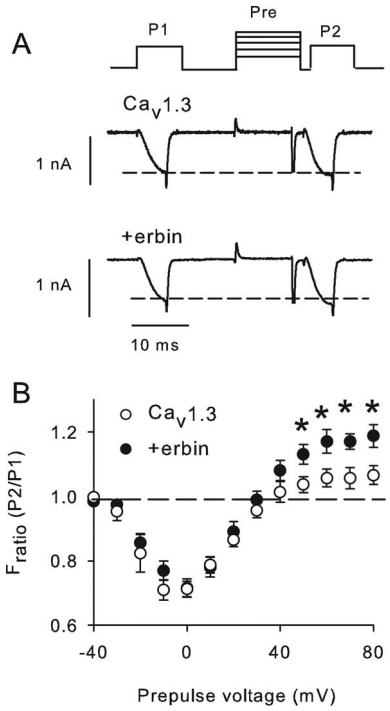

Figure 6. Erbin increases VDF of $Ca_v1.3$ Ca^{2+} currents. ***A***, Representative Ca^{2+} current traces and double-pulse voltage protocol for measuring VDF in cells transfected with $Ca_v1.3$ alone ($n = 6$) or cotransfected with erbin ($n = 7$). Currents were evoked by 5 ms test pulses from −90 to −10 mV before (P1) and after (P2) a conditioning 10 ms prepulse (Pre) to varying voltages. ***B***, Increased net facilitation for prepulse voltages greater than +40 mV in cells cotransfected with erbin. F_{ratio} was determined and plotted against prepulse voltage as in Figure 5*C*. The dotted line indicates $F_{ratio} = 1$. Points falling below the line result from Ca^{2+}-dependent inactivation with prepulse voltages evoking significant Ca^{2+} entry. *$p < 0.05$ by two-factor ANOVA and Tukey's post-test. Error bars represent SEM.

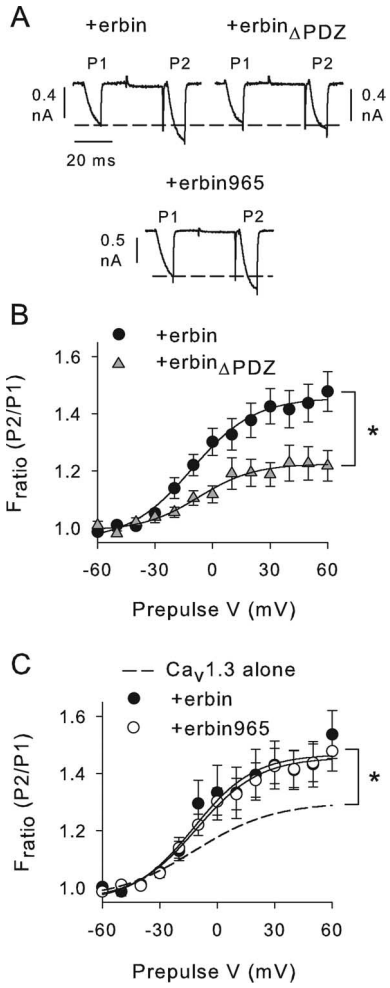

Figure 7. Increased VDF depends on PDZ domain of erbin. ***A***, Representative current traces obtained with the same voltage protocol as in Figure 5*A* for cells cotransfected with $Ca_v1.3$ plus erbin, erbin$_{\Delta PDZ}$, or erbin965 (amino acids 965–1371). ***B***, Deletion of erbinPDZ prevents effects on VDF. F_{ratio} is plotted against prepulse *V* for cells cotransfected with $Ca_v1.3$ plus erbin ($n = 10$) or erbin$_{\Delta PDZ}$ ($n = 8$). *$p < 0.05$. ***C***, Deletion of LRR of erbin does not prevent effects of erbin on VDF. F_{ratio} was plotted against prepulse voltage for cells cotransfected with $Ca_v1.3$ plus erbin ($n = 10$) or erbin965 ($n = 5$). The dashed line represents data replotted from Figure 5*C* for cells transfected with $Ca_v1.3$ alone. *$p < 0.05$ for $Ca_v1.3$ plus erbin965 compared with $Ca_v1.3$ alone. Error bars represent SEM.

Erbin interactions might facilitate voltage-dependent removal of the $\alpha_1$1.3 CT, thus disinhibiting VDF as in $Ca_v1.3b$ channels. If so, then CT_{500} should similarly "reinhibit" VDF of $Ca_v1.3$ channels modulated by erbin. As predicted, coexpression of CT_{500} strongly suppressed the increase in VDF caused by erbin ($F_{(1,19)} = 23.18$; $p < 0.001$) (Fig. 9*C*). However, in this experiment, VDF inhibition could have resulted simply from CT_{500} competitively binding to erbin and displacing it from the channel. This would then allow the endogenous CT of the channel to inhibit VDF, as in cells transfected with $Ca_v1.3$ alone. If this were the case, inhibition by CT_{500} in cells cotransfected with $Ca_v1.3$ plus erbin should be relatively invariant with prepulse voltage and similar to that seen in cells transfected with $Ca_v1.3$ alone. Alternatively, if CT_{500} inhibition involved interaction with an inhibitory site in $Ca_v1.3$ that was increasingly accessible in facilitated channels, CT_{500} inhibition in cells cotransfected with $Ca_v1.3$ plus erbin should increase with prepulse voltage, as in cells transfected with $Ca_v1.3b$ alone. To resolve the underlying mechanism, we compared the prepulse voltage dependence of VDF inhibition by CT_{500} for $Ca_v1.3$, $Ca_v1.3b$, and $Ca_v1.3$ plus erbin (Fig. 9*D*). In cells transfected with $Ca_v1.3$ plus erbin, VDF inhibition by CT_{500} increased steeply with prepulse voltage and was not significantly different from that in cells transfected with $Ca_v1.3b$ alone ($F_{(1,15)} = 0.29$; $p = 0.60$) (Fig. 9*D*). In contrast, percentage of inhibition of VDF by CT_{500} in cells with $Ca_v1.3$ alone did not vary greatly with prepulse voltage and was significantly different from that in cells with either $Ca_v1.3b$ ($F_{(1,8)} = 31.0$; $p < 0.001$) or with $Ca_v1.3$ plus erbin ($F_{(1,13)} = 25.0$; $p < 0.001$) (Fig. 9*D*). These results show that CT_{500} does not reverse the effects of erbin by displacing it from the channel. Rather, our data suggest that CT_{500} suppresses VDF in cells with $Ca_v1.3b$ or $Ca_v1.3$ plus erbin through the same voltage-dependent mechanism.

Because VDF of L-type channels can be affected by the auxiliary Ca^{2+} channel β subunit (Cens et al., 1998), we determined whether substituting the β_{1b} subunit used in our experiments with the β_4 subunit influenced modulation of $Ca_v1.3$ VDF by erbin and $\alpha_1$1.3 CT. Like β_{1b}, β_4 is highly expressed in the brain (Castellano et al., 1993; Ludwig et al., 1997; Vendel et al., 2006) and has been shown to associate with a large fraction of brain L-type channels (Pichler et al., 1997), although the identity of the β subunits interacting specifically with $Ca_v1.3$ in the brain has yet to be characterized. Although $Ca_v1.3$ channels containing β_4 ($Ca_v1.3$-β_4) exhibited VDF similar to that with β_{1b}, there was no significant difference in VDF in cells with $Ca_v1.3$-β_4 alone and those cotransfected with erbin ($F_{(1,13)} = 0.05$; $p = 0.83$) (Fig. 10*A*). However, VDF of the $Ca_v1.3b$ variant with β_4 ($Ca_v1.3b$-β_4) was significantly increased compared with $Ca_v1.3$-β_4 ($F_{(1,11)} =$

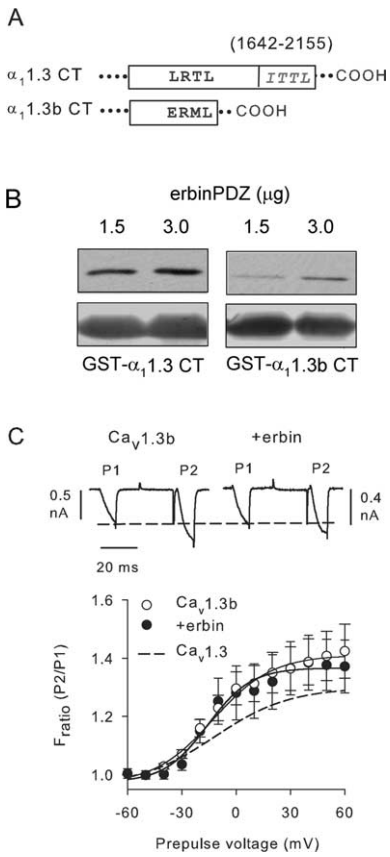

Figure 8. Erbin does not cause increased VDF of $Ca_v1.3b$ channels. ***A***, Schematic showing differences in C-terminal domain of $\alpha_1 1.3$ and $\alpha_1 1.3b$. Parentheses indicate unique sequence including the PDZ-binding site (ITTL) in $\alpha_1 1.3$ but not $\alpha_1 1.3b$. Splicing of this region in $\alpha_1 1.3b$ results in a truncated C-terminal domain with a distinct C-terminal sequence (ERML). ***B***, Erbin-PDZ interacts weakly with $\alpha_1 1.3b$ CT. GST-$\alpha_1 1.3$ CT or GST-$\alpha_1 1.3b$ CT was used in pull-down assay with his-S-erbinPDZ (1.5 or 3.0 μg). Top, Western blot detection of erbinPDZ. Bottom, Ponceau staining showing equal levels of immobilized GST-$\alpha_1 1.3$ CT (left) and GST-$\alpha_1 1.3b$ CT (right) used in assay. ***C***, No effect of erbin on VDF of $Ca_v1.3b$. F_{ratio} was plotted against prepulse voltage for cells transfected with $Ca_v1.3b$ alone ($n = 14$) or cotransfected with erbin ($n = 8$). The dashed line represents data replotted from Figure 5*C* for cells transfected with $Ca_v1.3$ alone. Representative current traces obtained with a +60 mV prepulse are shown above. Error bars represent SEM.

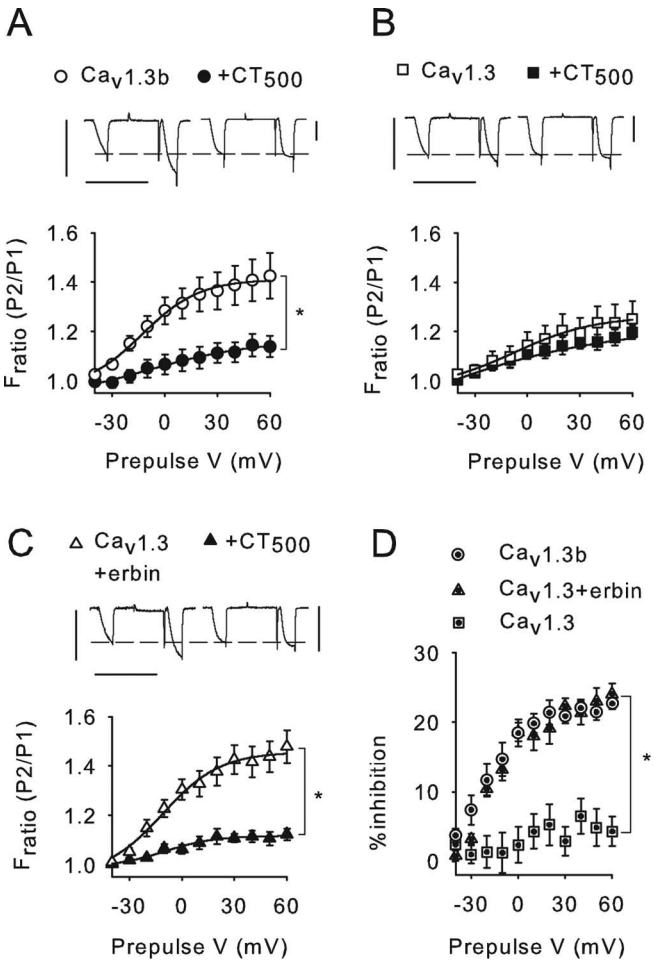

Figure 9. Autoinhibition of VDF by the CT of $\alpha_1 1.3$. ***A–C***, Cotransfection of $\alpha_1 1.3$ CT fragment (CT_{500}; amino acids 1655–2155) suppresses VDF. Effect of CT_{500} on F_{ratio} is plotted against prepulse *V* in cells with $Ca_v1.3b$ ($n = 6$) (***A***), $Ca_v1.3$ ($n = 4$; ***B***), or $Ca_v1.3$ plus erbin ($n = 10$; ***C***). Representative current traces obtained with a +60 mV prepulse are shown above. Vertical scale bars, 0.8 nA; horizontal scale bars, 40 ms. *$p < 0.01$. ***D***, Voltage-dependent inhibition of VDF by CT_{500}. Percentage inhibition was measured as $[1 - (F_{ratio+CT500}/F_{ratio})] \times 100$, where F_{ratio} is for $Ca_v1.3b$, $Ca_v1.3$, or $Ca_v1.3$ plus erbin, and $F_{ratio+CT500}$ represents the mean F_{ratio} for these groups cotransfected with CT_{500}. Stronger prepulse voltage dependence of CT_{500} inhibition is observed for $Ca_v1.3b$ and $Ca_v1.3$ plus erbin compared with $Ca_v1.3$. *$p < 0.001$. Error bars represent SEM.

13.8; $p < 0.01$) (Fig. 10*A*,*B*). Moreover, coexpression of CT_{500} with $Ca_v1.3b$-β_4 significantly blunted VDF ($F_{(1,11)} = 44.5$; $p < 0.001$) (Fig. 10*B*), similar to that observed for $Ca_v1.3b$ channels containing β_{1b} (Fig. 9*A*). We conclude that VDF modulation by erbin depends on which β subunit is associated with $Ca_v1.3$, and the inhibition of VDF imposed by the $\alpha_1 1.3$ CT is a fundamental regulatory feature of $\alpha_1 1.3$, which is removed by alternative splicing of the CT in $Ca_v1.3b$.

Discussion

Our results reveal a novel mechanism controlling VDF of $Ca_v1.3$ Ca^{2+} channels. Erbin binding to the CT of the $Ca_v1.3$ α_1 subunit alleviates an inhibitory effect of the CT, causing increased facilitation of $Ca_v1.3$ currents after a conditioning prepulse. This effect is seen for $Ca_v1.3$ channels containing the auxiliary β_{1b} but not β_4 subunit (Figs. 5*C*, 10*A*). The $Ca_v1.3b$ variant lacks the PDZ-binding site with which erbin interacts and, more importantly, the autoinhibitory CT domain. As a consequence, $Ca_v1.3b$ channels are "disinhibited," exhibiting more robust VDF than $Ca_v1.3$, regardless of the identity of the auxiliary β subunit (Figs. 8–10). Thus, the extent to which neuronal $Ca_v1.3$ channels undergo facilitation in response to membrane depolarization may depend on $\alpha_1 1.3$ splice variation and cell-type specific interactions with different β subunits and PDZ proteins.

Mechanisms of L-type channel facilitation

Facilitation of voltage-gated Ca^{2+} channels in response to a hormonal or depolarizing stimulus is an adaptive mechanism that can boost Ca^{2+} entry in excitable cells (Pietrobon and Hess, 1990; Dolphin, 1996). For $Ca_v1.2$ L-type channels, various mechanisms for facilitation have been characterized, including those involving phosphorylation of the channel by cAMP-dependent protein kinase (PKA) (Catterall, 2000) and association with calmodulin-dependent protein kinase II (CaMKII) (Dzhura et al., 2000; Hudmon et al., 2005; Grueter et al., 2006; Lee et al., 2006). Although PKA and CaMKII also cause facilitation of $Ca_v1.3$ channels (Qu et al., 2005; Gao et al., 2006), the enhanced facilitation caused by erbin and splice variation of the $\alpha_1 1.3$ CT in our study differs from these mechanisms in a number of ways. First, although PKA and CaMKII cause an increase in $Ca_v1.3$ peak

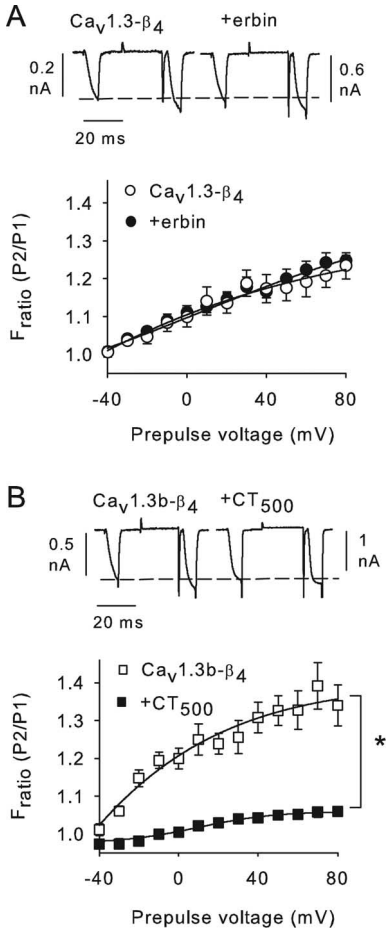

Figure 10. Effect of erbin but not $\alpha_1$1.3 CT depends on auxiliary Ca^{2+} channel β subunit. ***A***, Erbin does not increase VDF of $Ca_v1.3$ channels containing the β_4 subunit ($Ca_v1.3$-β_4). F_{ratio} was determined from double-pulse protocol as described in Figure 5, except that P1 and P2 currents were evoked by 7 ms test pulses from −90 to −20 mV in cells transfected with $Ca_v1.3$-β_4 ($n = 7$) or cotransfected with erbin ($n = 8$). ***B***, CT_{500} inhibits VDF of β_4-containing $Ca_v1.3b$ channels ($Ca_v1.3b$-β_4). F_{ratio} was determined and plotted as in ***A*** for cells transfected with $Ca_v1.3b$-β_4 ($n = 6$) or cotransfected with CT_{500} ($n = 7$). *$p < 0.001$. For ***A*** and ***B***, representative current traces obtained with +80 mV prepulse are shown above. Error bars represent SEM.

current amplitude (Qu et al., 2005) and negative shift in voltage-dependent activation (Gao et al., 2006), respectively, erbin had neither effect on $Ca_v1.3$ activation in our study (Fig. 4). Second, CaMKII activation by insulin-like growth factor causes facilitation of both $Ca_v1.3$ and $Ca_v1.3b$ (Gao et al., 2006), whereas we find that $Ca_v1.3$ but not $Ca_v1.3b$ channels are subject to erbin-dependent facilitation (Figs. 5, 8). Third, neither PKA nor CaMKII-dependent facilitation of $Ca_v1.3$ requires conditioning depolarization (Qu et al., 2005; Gao et al., 2006), unlike the clearly voltage-dependent effects of erbin on $Ca_v1.3$ facilitation (Fig. 5). Therefore, we conclude that erbin promotes facilitation of $Ca_v1.3$ channels via a different molecular pathway than that described previously for these channels by PKA or CaMKII. Although we cannot rule out the possibility that other second messengers are involved, our data implicate the $\alpha_1$1.3 CT as a key regulatory element in this process.

Autoinhibitory function of the $\alpha_1$1.3 CT and modulation by PDZ proteins

An autoinhibitory role for the CT of the $Ca_v1.1$ and $Ca_v1.2$ α_1 subunits is well established (Wei et al., 1994; Morrill and Cannon, 2000; Gao et al., 2001). Deletion of the distal C-terminal domain of the α_1 subunit enhances activation of $Ca_v1.1$ (Morrill and Cannon, 2000) and $Ca_v1.2$ (Wei et al., 1994) when these channels are expressed in recombinant systems. This upregulation of channel activity is reversed by reintroduction of the distal CT fragment as a separate entity (Gao et al., 2001; Hulme et al., 2005, 2006), much like the inhibitory effects on VDF that we observed when the $\alpha_1$1.3 CT (CT_{500}) was coexpressed with $Ca_v1.3b$ (Figs. 9*A*,*D*, 10*B*) or $Ca_v1.3$ plus erbin (Fig. 9*C*,*D*). How the $\alpha_1$1.3 CT inhibits VDF is not clear but may involve intramolecular interactions with other domains in $\alpha_1$1.3. Previous studies have shown that the CT of $\alpha_1$1.2 and $\alpha_1$1.1 is subject to proteolytic processing *in vivo* (De Jongh et al., 1991; Hell et al., 1993a) and that the cleaved distal CT product remains associated with the α_1 subunit (Gerhardstein et al., 2000; Hulme et al., 2005, 2006). For $Ca_v1.1$ and $Ca_v1.2$, the distal CT interacts directly with the proximal CT of the α_1 subunit at sites that are conserved in the corresponding regions of $\alpha_1$1.3 (Hulme et al., 2005, 2006). The putative proximal CT interaction site is included in the CT_{500} fragment that inhibited VDF in our study (Figs. 9, 10*B*), whereas the distal CT interaction site is retained in the truncated CT of the $\alpha_1$1.3b (Fig. 8*A*). Thus, it is possible that for $Ca_v1.3$, the interaction of distal and proximal CT sites forms an autoinhibitory module for VDF, which is disrupted when erbin binds to the distal CT of β_{1b}-containing channels or when the distal CT is removed by alternative splicing in $Ca_v1.3b$. Coexpression of the CT_{500} fragment would inhibit VDF of $Ca_v1.3b$ (Figs. 9*A*,*D*, 10*B*) or $Ca_v1.3$ plus erbin (Fig. 9*C*,*D*) through reassociation with the proximal CT, therefore restoring the autoinhibition. Although additional experiments are required to confirm this mechanism, our results are consistent with previous observations that interdomain interactions involving the $\alpha_1$1.2 CT regulate $Ca_v1.2$ activation and inactivation (Ivanina et al., 2000; Kobrinsky et al., 2005), which might parallel the role of the CT in modulating $Ca_v1.3$ VDF.

Our findings that the $Ca_v1.3$ channels containing the β_4 subunit were insensitive to modulation by erbin further underscore the importance of auxiliary β subunits in differentially regulating not only gating but also modulation of voltage-gated Ca^{2+} channels (Richards et al., 2004). Although additional investigation is necessary, β_4 may impair physical association of erbin with $Ca_v1.3$ or channel transitions to facilitated states that are favored by erbin. Alternatively, given that β_4 variants interact with cellular signaling molecules other than voltage-gated Ca^{2+} channels (Hibino et al., 2003; Vendel et al., 2006), β_4 could recruit other modulators to the $Ca_v1.3$ channel complex that oppose the effects of erbin. Because both β_{1b} and β_4 are highly expressed in the brain (Ludwig et al., 1997; Pichler et al., 1997), whether neuronal $Ca_v1.3$ channels are modulated by erbin could vary according to which β subunit is associated with the channel complex.

PDZ proteins as modulators of voltage-gated Ca^{2+} channels

PDZ domain-containing proteins have emerged as multifaceted regulators of voltage-gated Ca^{2+} channel targeting and localization (Maximov et al., 1999; Zhang et al., 2005, 2006), modulation by G-protein-coupled receptors (Olson et al., 2005), and signal transduction (Weick et al., 2003). By selectively targeting and assembling Ca^{2+} channels with various signaling molecules, PDZ proteins can confer specific forms of Ca^{2+} channel regulation in different subcellular contexts. For example, the PDZ protein Shank clusters $Ca_v1.3$ but not $Ca_v1.2$ at postsynaptic sites with D_1 dopamine receptors, enabling dopaminergic suppression of $Ca_v1.3$ L-type currents (Olson et al., 2005; Zhang et al., 2005). Our study is the first to show a more direct role for a PDZ protein in regulating Ca^{2+} channel gating. We have not tested whether

related PDZ proteins, such as Shank, that interact with the $\alpha_1$1.3 CT have an effect similar to erbin in increasing VDF of $Ca_v1.3$-β_{1b}. Our findings that a truncated version of erbin containing primarily the PDZ domain ($erbin_{965}$) (Fig. 7*A*,*C*) was sufficient for increasing VDF suggest that a PDZ/$\alpha_1$1.3 CT interaction is the essential determinant for the modulation. However, PDZ proteins, including erbin and Shank, differ significantly in their overall structure and can vary in terms of the number of PDZ domains and the existence of other protein interaction motifs (Kim and Sheng, 2004). Such structural variations may alter the modulatory potential of PDZ proteins, perhaps by allowing them to scaffold multiple distinct signaling molecules. This raises the possibility that a wide range of PDZ interactions may influence other aspects of $Ca_v1.3$ function, thus enhancing the signaling capabilities of these channels in neurons. In this context, it is important to note that peptide mimetics of the class I PDZ-binding site in $\alpha_1$1.3 (Fig. 1*A*) may competitively disrupt interactions with multiple PDZ proteins and thus may not reflect the functional consequences of disturbing a single PDZ interaction.

Physiological significance of $Ca_v1.3$ channel facilitation and modulation by erbin/$\alpha_1$1.3 splicing

Compared with previous descriptions of native L-type channel VDF (Pietrobon and Hess, 1990; Forti and Pietrobon, 1993; Kavalali and Plummer, 1996), VDF of $Ca_v1.3$ channels in our experiments occurred with relatively moderate depolarizing prepulses (−20 to +60 mV) (Figs. 5–10). This feature of VDF is consistent with previous reports of $Ca_v1.3$ splice variants cloned from a pituitary cell line (Safa et al., 2001) and L-type channels in neostriatal medium spiny neurons (Song and Surmeier, 1996) and hippocampal pyramidal neurons (Kavalali and Plummer, 1996). In cortical neurons, L-type channels influence neuronal activity via Ca^{2+}-dependent plateau potentials (Nasif et al., 2005) and regulation of interspike intervals during repetitive firing (Pineda et al., 1998). Increased VDF of $Ca_v1.3$-β_{1b} caused by erbin or expression of the $Ca_v1.3b$ variant could amplify such activity-dependent Ca^{2+} signals, which normally control cortical excitability. Given that $Ca_v1.3$-β_{1b} but not $Ca_v1.3$-β_4 channels are subject to modulation by erbin (Figs. 5, 10), it is interesting to consider the lethargic mutation in the Ca^{2+} channel β_4 subunit, which causes seizures and ataxia (Burgess et al., 1997). This mutation prevents interactions of β_4 with the Ca^{2+} channel α_1 subunit and causes compensatory increases in the association of α_1 with other β subunits, including β_{1b} (Burgess et al., 1999). Our results suggest a mechanism in which such pathological increases in $Ca_v1.3$-β_{1b} channels might cause neurological defects through aberrant upregulation of Ca^{2+} signaling and neuronal excitability.

References

Bading H, Ginty DD, Greenberg ME (1993) Regulation of gene expression in hippocampal neurons by distinct calcium signaling pathways. Science 260:181–186.

Borg JP, Marchetto S, Le Bivic A, Ollendorff V, Jaulin-Bastard F, Saito H, Fournier E, Adelaide J, Margolis B, Birnbaum D (2000) ERBIN: a basolateral PDZ protein that interacts with the mammalian ERBB2/HER2 receptor. Nat Cell Biol 2:407–414.

Burgess DL, Jones JM, Meisler MH, Noebels JL (1997) Mutation of the Ca^{2+} channel β subunit gene *Cchb4* is associated with ataxia and seizures in the lethargic (*lh*) mouse. Cell 88:385–392.

Burgess DL, Biddlecome GH, McDonough SI, Diaz ME, Zilinski CA, Bean BP, Campbell KP, Noebels JL (1999) β subunit reshuffling modifies N- and P/Q-type Ca^{2+} channel subunit compositions in lethargic mouse brain. Mol Cell Neurosci 13:293–311.

Castellano A, Wei X, Birnbaumer L, Perez-Reyes E (1993) Cloning and expression of a neuronal calcium channel β subunit. J Biol Chem 268:12359–12366.

Catterall WA (2000) Structure and regulation of voltage-gated Ca^{2+} channels. Annu Rev Cell Dev Biol 16:521–555.

Cens T, Restituito S, Vallentin A, Charnet P (1998) Promotion and inhibition of L-type Ca^{2+} channel facilitation by distinct domains of the β subunit. J Biol Chem 273:18308–18315.

Dai P, Xiong WC, Mei L (2006) Erbin inhibits RAF activation by disrupting the sur-8-Ras-Raf complex. J Biol Chem 281:927–933.

Day M, Wang Z, Ding J, An X, Ingham CA, Shering AF, Wokosin D, Ilijic E, Sun Z, Sampson AR, Mugnaini E, Deutch AY, Sesack SR, Arbuthnott GW, Surmeier DJ (2006) Selective elimination of glutamatergic synapses on striatopallidal neurons in Parkinson disease models. Nat Neurosci 9:251–259.

De Jongh KS, Warner C, Colvin AA, Catterall WA (1991) Characterization of the two size forms of the α1 subunit of skeletal muscle L-type calcium channels. Proc Natl Acad Sci USA 88:10778–10782.

Dolphin AC (1996) Facilitation of Ca^{2+} current in excitable cells. Trends Neurosci 19:35–43.

Dou H, Vazquez AE, Namkung Y, Chu H, Cardell EL, Nie L, Parson S, Shin HS, Yamoah EN (2004) Null mutation of α1D Ca^{2+} channel gene results in deafness but no vestibular defect in mice. J Assoc Res Otolaryngol 5:215–226.

Dzhura I, Wu Y, Colbran RJ, Balser JR, Anderson ME (2000) Calmodulin kinase determines calcium-dependent facilitation of L-type calcium channels. Nat Cell Biol 2:173–177.

Fam SR, Paquet M, Castleberry AM, Oller H, Lee CJ, Traynelis SF, Smith Y, Yun CC, Hall RA (2005) P2Y1 receptor signaling is controlled by interaction with the PDZ scaffold NHERF-2. Proc Natl Acad Sci USA 102:8042–8047.

Forti L, Pietrobon D (1993) Functional diversity of L-type calcium channels in rat cerebellar neurons. Neuron 10:437–450.

Gao L, Blair LA, Salinas GD, Needleman LA, Marshall J (2006) Insulin-like growth factor-1 modulation of $Ca_V1.3$ calcium channels depends on Ca^{2+} release from IP3-sensitive stores and calcium/calmodulin kinase II phosphorylation of the α1 subunit EF hand. J Neurosci 26:6259–6268.

Gao T, Cuadra AE, Ma H, Bunemann M, Gerhardstein BL, Cheng T, Eick RT, Hosey MM (2001) C-terminal fragments of the alpha 1C (CaV1.2) subunit associate with and regulate L-type calcium channels containing C-terminal-truncated alpha 1C subunits. J Biol Chem 276:21089–21097.

Gerhardstein BL, Gao T, Bunemann M, Puri TS, Adair A, Ma H, Hosey MM (2000) Proteolytic processing of the C terminus of the α_{1C} subunit of L-type calcium channels and the role of a proline-rich domain in membrane tethering of proteolytic fragments. J Biol Chem 275:8556–8563.

Grueter CE, Abiria SA, Dzhura I, Wu Y, Ham AJ, Mohler PJ, Anderson ME, Colbran RJ (2006) L-type Ca^{2+} channel facilitation mediated by phosphorylation of the beta subunit by CaMKII. Mol Cell 23:641–650.

Hell JW, Yokoyama CT, Wong ST, Warner C, Snutch TP, Catterall WA (1993a) Differential phosphorylation of two size forms of the neuronal class C L-type calcium channel α1 subunit. J Biol Chem 268:19451–19457.

Hell JW, Westenbroek RE, Warner C, Ahlijanian MK, Prystay W, Gilbert MM, Snutch TP, Catterall WA (1993b) Identification and differential subcellular localization of the neuronal class C and class D L-type calcium channel alpha 1 subunits. J Cell Biol 123:949–962.

Hetzenauer A, Sinnegger-Brauns MJ, Striessnig J, Singewald N (2006) Brain activation pattern induced by stimulation of L-type Ca^{2+}-channels: contribution of $Ca_V1.3$ and $Ca_V1.2$ isoforms. Neuroscience 139:1005–1015.

Hibino H, Pironkova R, Onwumere O, Rousset M, Charnet P, Hudspeth AJ, Lesage F (2003) Direct interaction with a nuclear protein and regulation of gene silencing by a variant of the Ca^{2+}-channel β_4 subunit. Proc Natl Acad Sci USA 100:307–312.

Huang YZ, Wang Q, Xiong WC, Mei L (2001) Erbin is a protein concentrated at postsynaptic membranes that interacts with PSD-95. J Biol Chem 276:19318–19326.

Hudmon A, Schulman H, Kim J, Maltez JM, Tsien RW, Pitt GS (2005) CaMKII tethers to L-type Ca^{2+} channels, establishing a local and dedicated integrator of Ca^{2+} signals for facilitation. J Cell Biol 171:537–547.

Hulme JT, Konoki K, Lin TW, Gritsenko MA, Camp II DG, Bigelow DJ, Catterall WA (2005) Sites of proteolytic processing and noncovalent association of the distal C-terminal domain of Ca_V 1.1 channels in skeletal muscle. Proc Natl Acad Sci USA 102:5274–5279.

Hulme JT, Yarov-Yarovoy V, Lin TW, Scheuer T, Catterall WA (2006) Au-

toinhibitory control of the CaV1.2 channel by its proteolytically processed distal C-terminal domain. J Physiol (Lond) 576:87–102.
Ivanina T, Blumenstein Y, Shistik E, Barzilai R, Dascal N (2000) Modulation of L-type Ca^{2+} channels by $G\beta\gamma$ and calmodulin via interactions with N and C termini of alpha 1C. J Biol Chem 275:39846–39854.
Jaulin-Bastard F, Saito H, Le Bivic A, Ollendorff V, Marchetto S, Birnbaum D, Borg JP (2001) The ERBB2/HER2 receptor differentially interacts with ERBIN and PICK1 PSD-95/DLG/ZO-1 domain proteins. J Biol Chem 276:15256–15263.
Johnston D, Williams S, Jaffe D, Gray R (1992) NMDA-receptor-independent long-term potentiation. Annu Rev Physiol 54:489–505.
Kavalali ET, Plummer MR (1996) Multiple voltage-dependent mechanisms potentiate calcium channel activity in hippocampal neurons. J Neurosci 16:1072–1082.
Kim E, Sheng M (2004) PDZ domain proteins of synapses. Nat Rev Neurosci 5:771–781.
Kobrinsky E, Tiwari S, Maltsev V, Harry JB, Lakatta E, Abernethy DR, Soldatov NM (2005) Differential role of the alpha 1C subunit tails in regulation of the $Ca_v1.2$ channel by membrane potential, beta subunits and Ca^{2+} ions. J Biol Chem 280:12474–12485.
Kolch W (2003) Erbin: sorting out ErbB2 receptors or giving Ras a break? Sci STKE 2003:37.
Koschak A, Reimer D, Huber I, Grabner M, Glossmann H, Engel J, Striessnig J (2001) α_{1D} ($Ca_v1.3$) subunits can form L-type Ca^{2+} channels activating at negative voltages. J Biol Chem 276:22100–22106.
Lee TS, Karl R, Moosmang S, Lenhardt P, Klugbauer N, Hofmann F, Kleppisch T, Welling A (2006) Calmodulin kinase II is involved in voltage-dependent facilitation of the L-type $Ca_v1.2$ calcium channel: identification of the phosphorylation sites. J Biol Chem 281:25560–25567.
Legouis R, Jaulin-Bastard F, Schott S, Navarro C, Borg JP, Labouesse M (2003) Basolateral targeting by leucine-rich repeat domains in epithelial cells. EMBO Rep 4:1096–1102.
Ludwig A, Flockerzi V, Hofmann F (1997) Regional expression and cellular localization of the α_1 and β subunit of high voltage-activated calcium channels in rat brain. J Neurosci 17:1339–1349.
Marrion NV, Tavalin SJ (1998) Selective activation of Ca^{2+}-activated K^+ channels by co-localized Ca^{2+} channels in hippocampal neurons. Nature 395:900–905.
Maximov A, Sudhof TC, Bezprozvanny I (1999) Association of neuronal calcium channels with modular adaptor proteins. J Biol Chem 274:24453–24456.
Moosmang S, Haider N, Klugbauer N, Adelsberger H, Langwieser N, Muller J, Stiess M, Marais E, Schulla V, Lacinova L, Goebbels S, Nave KA, Storm DR, Hofmann F, Kleppisch T (2005) Role of hippocampal $Ca_v1.2$ Ca^{2+} channels in NMDA receptor-independent synaptic plasticity and spatial memory. J Neurosci 25:9883–9892.
Morrill JA, Cannon SC (2000) COOH-terminal truncated α_{1S} subunits conduct current better than full-length dihydropyridine receptors. J Gen Physiol 116:341–348.
Nasif FJ, Hu XT, White FJ (2005) Repeated cocaine administration increases voltage-sensitive calcium currents in response to membrane depolarization in medial prefrontal cortex pyramidal neurons. J Neurosci 25:3674–3679.
Olson PA, Tkatch T, Hernandez-Lopez S, Ulrich S, Ilijic E, Mugnaini E, Zhang H, Bezprozvanny I, Surmeier DJ (2005) G-protein-coupled receptor modulation of striatal $Ca_V1.3$ L-type Ca^{2+} channels is dependent on a Shank-binding domain. J Neurosci 25:1050–1062.
Ou Y, Strege P, Miller SM, Makielski J, Ackerman M, Gibbons SJ, Farrugia G (2003) Syntrophin gamma 2 regulates SCN5A gating by a PDZ domain-mediated interaction. J Biol Chem 278:1915–1923.
Penkert RR, DiVittorio HM, Prehoda KE (2004) Internal recognition through PDZ domain plasticity in the Par-6-Pals1 complex. Nat Struct Mol Biol 11:1122–1127.
Pichler M, Cassidy TN, Reimer D, Haase H, Krause R, Ostler D, Striessnig J (1997) β subunit heterogeneity in neuronal L-type Ca^{2+} channels. J Biol Chem 272:13877–13882.
Pietrobon D, Hess P (1990) Novel mechanism of voltage-dependent gating in L-type calcium channels. Nature 346:651–655.
Pineda JC, Waters RS, Foehring RC (1998) Specificity in the interaction of HVA Ca^{2+} channel types with Ca^{2+}-dependent AHPs and firing behavior in neocortical pyramidal neurons. J Neurophysiol 79:2522–2534.
Platzer J, Engel J, Schrott-Fischer A, Stephan K, Bova S, Chen H, Zheng H, Striessnig J (2000) Congenital deafness and sinoatrial node dysfunction in mice lacking class D L-type Ca^{2+} channels. Cell 102:89–97.
Qu Y, Baroudi G, Yue Y, El-Sherif N, Boutjdir M (2005) Localization and modulation of α_{1D} ($Ca_v1.3$) L-type Ca^{2+} channel by protein kinase A. Am J Physiol Heart Circ Physiol 288:H2123–H2130.
Richards MW, Butcher AJ, Dolphin AC (2004) Ca^{2+} channel β-subunits: structural insights AID our understanding. Trends Pharmacol Sci 25:626–632.
Safa P, Boulter J, Hales TG (2001) Functional properties of $Ca_v1.3$ (alpha1D) L-type Ca^{2+} channel splice variants expressed by rat brain and neuroendocrine GH3 cells. J Biol Chem 276:38727–38737.
Scholze A, Plant TD, Dolphin AC, Nurnberg B (2001) Functional expression and characterization of a voltage-gated $Ca_V1.3$ (α_{1D}) calcium channel subunit from an insulin-secreting cell line. Mol Endocrinol 15:1211–1221.
Sinnegger-Brauns MJ, Hetzenauer A, Huber IG, Renstrom E, Wietzorrek G, Berjukov S, Cavalli M, Walter D, Koschak A, Waldschutz R, Hering S, Bova S, Rorsman P, Pongs O, Singewald N, Striessnig J (2004) Isoform-specific regulation of mood behavior and pancreatic beta cell and cardiovascular function by L-type Ca^{2+} channels. J Clin Invest 113:1430–1439.
Song WJ, Surmeier DJ (1996) Voltage-dependent facilitation of calcium channels in rat neostriatal neurons. J Neurophysiol 76:2290–2306.
Songyang Z, Fanning AS, Fu C, Xu J, Marfatia SM, Chishti AH, Crompton A, Chan AC, Anderson JM, Cantley LC (1997) Recognition of unique carboxyl-terminal motifs by distinct PDZ domains. Science 275:73–77.
Vendel AC, Terry MD, Striegel AR, Iverson NM, Leuranguer V, Rithner CD, Lyons BA, Pickard GE, Tobet SA, Horne WA (2006) Alternative splicing of the voltage-gated Ca^{2+} channel β_4 subunit creates a uniquely folded N-terminal protein binding domain with cell-specific expression in the cerebellar cortex. J Neurosci 26:2635–2644.
Wei X, Neely A, Lacerda AE, Olcese R, Stefani E, Perez-Reyes E, Birnbaumer L (1994) Modification of Ca^{2+} channel activity by deletions at the carboxyl terminus of the cardiac α_1 subunit. J Biol Chem 269:1635–1640.
Weick JP, Groth RD, Isaksen AL, Mermelstein PG (2003) Interactions with PDZ proteins are required for L-type calcium channels to activate cAMP response element-binding protein-dependent gene expression. J Neurosci 23:3446–3456.
Xu W, Lipscombe D (2001) Neuronal $Ca(V)1.3\alpha_1$ L-type channels activate at relatively hyperpolarized membrane potentials and are incompletely inhibited by dihydropyridines. J Neurosci 21:5944–5951.
Zhang H, Maximov A, Fu Y, Xu F, Tang TS, Tkatch T, Surmeier DJ, Bezprozvanny I (2005) Association of $Ca_V1.3$ L-type calcium channels with Shank. J Neurosci 25:1037–1049.
Zhang H, Fu Y, Altier C, Platzer J, Surmeier DJ, Bezprozvanny I (2006) $Ca_V1.2$ and $Ca_V1.3$ neuronal L-type calcium channels: differential targeting and signaling to pCREB. Eur J Neurosci 23:2297–2310.
Zhou H, Kim SA, Kirk EA, Tippens AL, Sun H, Haeseleer F, Lee A (2004) Ca^{2+}-binding protein-1 facilitates and forms a postsynaptic complex with $Ca_v1.2$ (L-type) Ca^{2+} channels. J Neurosci 24:4698–4708.